EXPERIMENTAL INVESTIGATION OF REFRIGERATOR CONDENSERS FOR POSSIBLE DESIGN IMPROVEMENTS

A THESIS SUBMITTED TO

THE GRADUATE SCHOOL OF NATURAL AND APPLIED SCIENCES

OF

MIDDLE EAST TECHNICAL UNIVERSITY

BY

NEJDET YİĞİT ÖZSAÇMACI

IN PARTIAL FULFILLMENT OF THE REQUIREMENTS

FOR

THE DEGREE OF MASTER OF SCIENCE

IN

MECHANICAL ENGINEERING

JUNE 2014

Approval of the thesis:

EXPERIMENTAL INVESTIGATION OF REFRIGERATOR CONDENSERS FOR POSSIBLE DESIGN IMPROVEMENTS

Submitted by **NEJDET YİĞİT ÖZSAÇMACI** in partial fulfillment of the requirements for the degree of **Master of Science in Mechanical Engineering Department, Middle East Technical University** by,

Prof. Dr. Canan ÖZGEN _____
Dean, Graduate School of **Natural and Applied Sciences**

Prof. Dr. Süha ORAL _____
Head of Department, **Mechanical Engineering, METU**

Assoc. Prof. Dr. Tuba OKUTUCU ÖZYURT _____
Supervisor, **Mechanical Engineering Department, METU**

Prof. Dr. Rüknettin OSKAY _____
Co-supervisor, **Mechanical Engineering Department, METU**

METU Examining Committee Members:

Assoc. Prof. Dr. Tuba OKUTUCU ÖZYURT _____
Mechanical Engineering Dept., METU

Prof. Dr. Rüknettin OSKAY _____
Mechanical Engineering Dept., METU

Assoc. Prof. Dr. Ahmet YOZGATLIGİL _____
Mechanical Engineering Dept., METU

Asst. Prof. Dr. Özgür BAYER _____
Mechanical Engineering Dept., METU

Dr. Tuğba SARIÇAY, Arçelik A.Ş. _____

Date: _____

I hereby declare that all information in this document has been obtained and presented in accordance with academic rules and ethical conduct. I also declare that, as required by these rules and conduct, I have fully cited and referenced all material and results that are not original to this work.

Name, Surname: Nejdet Yiğit OZSAÇMACI

Signature:

ABSTRACT

EXPERIMENTAL INVESTIGATION OF REFRIGERATOR CONDENSERS FOR POSSIBLE DESIGN IMPROVEMENTS

Özsaçmacı, Nejdet Yiğit

M.S., Department of Mechanical Engineering

Supervisor: Assoc. Prof. Dr. Tuba Okutucu Özyurt

Co-Supervisor: Prof. Dr. Rüknettin Oskay

June 2014, 83 pages

There is a continuous increase in the capacities of competitive markets in refrigeration industry. Meanwhile, new energy regulations for domestic appliances, including refrigerators become operative day by day. Hence, there is a strong requirement for improved performance of household refrigerators at reduced cost. The condenser is the main heat rejection component of the cooling cycle.

The objective of this thesis is to conduct an experimental investigation for possible design improvements of wire-and-tube type refrigerator condensers. The experiments were held in the laboratories of Arçelik Refrigerator Plant in Eskişehir. In addition to standard performance tests, charge experiments, 43ºC tropical climate tests, and not door opening (NDO) experiments were performed. Temperature and pressure measurements were carried out with thermocouples and pressure transducers, respectively. The data collection was performed by a data acquisition system.

The correlations for the refrigerant side heat transfer coefficients are obtained from the literature. Heat transfer rates are calculated with the help isobutane property tables and *P-h* diagram. Air side heat transfer coefficient is expressed in terms of convection only. Inside and outside convective heat transfer coefficients are calculated. The overall heat transfer coefficients are calculated and compared for different condenser configurations. Radiative effects are not considered in this study.

In the scope of the thesis, three different sets of experiments have been conducted. In the first and the third sets, a test chamber has been used to investigate the effects of different condenser configurations on refrigerator energy consumption. In the second part of the study an experimental setup was used to investigate the performance characteristics of a variety of wire-and tube type refrigerator condensers.

Experimental studies indicated that it is possible to save material and reduce the production cost by using shorter tubes of 4.76 mm diameter or tubes of 4 mm diameter without any loss in the thermal performance or increase in the energy consumption.

Keywords: Wire-and-tube type heat exchangers, natural convection, condenser, refrigerator, vapor compression refrigeration cycle.

ÖZ

OLASI TASARIM İYİLEŞTİRMELERİ İÇİN BUZDOLABI KONDENSERLERİNİN DENEYSEL İNCELENMESİ

Özsaçmacı, Nejdet Yiğit

Yüksek Lisans, Makina Mühendisliği Bölümü

Tez Yöneticisi: Doç. Dr. Tuba Okutucu Özyurt

Ortak Tez Yöneticisi: Prof. Dr. Rüknettin Oskay

Haziran 2014, 83 sayfa

Günümüzde soğutma sektöründe rekabetçi piyasaların kapasiteleri sürekli bir artış göstermektedir. Bu arada, buzdolabı gibi ev cihazlarında, her geçen gün yeni enerji düzenlemeleri yürürlüğe koyulmaktadır. Bu nedenle, düşük maliyetlerle buzdolaplarını daha iyi bir performans sağlayacak biçimde üretme gereksinimi doğmaktadır. Kondenser, soğutma çevriminin dışarıya ısı atan temel elemanıdır.

Bu tezin amacı, tel ve boru tipi buzdolabı kondenserlerini olası tasarım iyileştirmeleri için deneysel olarak incelemektir. Deneyler, Eskişehir Arçelik Buzdolabı İşletmesi laboratuvarlarında yapılmıştır. Standart performans testleri, şarj deneyleri, 43ºC tropik iklim testleri, kapı açma kapama deneyleri sırasıyla gerçekleştirilmiştir. Sıcaklık ve basınç ölçümleri sırasıyla, ısıl çift ve basınç algılayıcıları ile yapılmıştır. Deneysel veriler bir veri toplama sistemi aracılığıyla toplanmıştır.

Soğutkan tarafı ısı transfer katsayısı hesaplamaları için gereken bağıntılar literatürden elde edilmiştir. Isı transfer miktarı, izobütan özellik tabloları ve *P-h* diyagramları yardımı ile hesaplanmıştır. Hava tarafı ısı transfer katsayısı yalnızca taşınım bileşeni ile ifade edilmiştir. Tez çalışması kapsamında, boru içi ve hava tarafında taşınım ısı transfer katsayıları ile toplam ısı transfer katsayıları, farklı kondenser alternatifleri için hesaplanmış ve karşılaştırılmıştır. Tez çalışmasında ışınım etkileri değerlendirilmemiştir.

Tez kapsamında üç farklı set deney yapılmıştır. Birinci ve üçüncü set deneylerde farklı kondenser yapılanmalarının buzdolabı enerji tüketimine etkileri Minitab istatistik programı yardımı ile incelenmiştir. Çalışmanın ikinci bölümünde buzdolabı kondenserlerinin performans ölçümleri gerçekleştirilmiş ve farklı kondanser yapılanmaları için karşılaştırılmıştır.

Deney sonuçları, ısıl performans ve enerji tüketiminden ödün vermeden, kondenserde 4.76 mm çaplı ancak kısaltılmış borular, veya 4 mm çaplı borular kullanarak malzemeden ve maliyetten tasarruf edilebileceğini göstermiştir.

Anahtar Kelimeler: Tel ve boru tipi ısı değiştirgeci, doğal taşınım, kondenser, buzdolabı, buhar sıkıştırmalı soğutma çevrimi.

ACKNOWLEDGMENTS

I would like to express my sincere thanks to my supervisor, Assoc. Prof. Dr. Tuba OKUTUCU ÖZYURT, for her continuous guidance, support throughout the course of this thesis. I would also like to thank my co-supervisor Prof. Dr. Rüknettin OSKAY for his guidance, warnings and patience throughout the thesis study.

I would like to express my sincere appreciation to my colleagues at ARÇELIK refrigerator plant research and development department Yüksel ATİLLA, Veysi ERCAN, Fatih DEMİRAY, Dr. Tuğba SARIÇAY for their support, crucial advices during the preparation of this thesis. I would like to thank ARÇELİK A.Ş. for providing facilities for the experimental investigations. The help, encouragement and patience of all my colleagues throughout experiments are particularly appreciated.

I would like to thank my colleagues at ARÇELIK central research and development department, specifically Tolga APAYDIN and Vasi Kadir ERTİŞ for their support, suggestions and comments in this thesis. Their contributions are greatly appreciated and are respectfully acknowledged.

I would like to express my deepest thanks to my family for their endless support, love and faith. The help and encouragement of my sister Gözde ÖZSAÇMACI throughout the research are particularly appreciated.

TABLE OF CONTENTS

ABSTRACT..... v
ÖZ..... vii
ACKNOWLEDGMENTS..... ix
TABLE OF CONTENTS.....x
LIST OF TABLES xii
LIST OF FIGURES..... xiv
LIST OF SYMBOLS..... xvii
CHAPTERS
1. INTRODUCTION 1
1.1 Motivation.....1
1.2 Air-Cooled Condensers…….....5
1.3 Present Study 6
1.4 Thesis Outline.....6
2. LITERATURE REVIEW.....7
3. EXPERIMENTAL PROCEDURE.....17
3.1 Experimental Setup for the Refrigerator Tests.....17
3.2 Experimental Procedure for the Refrigerator Tests… 20
3.2.1 Optimization Test for the Amount of Refrigerant.....24
3.2.2 Refrigerator Energy Efficiency Class Determination.....24
3.2.3 Refrigerator Energy Measurement Test…….....28
3.3 Experimental Setup for Solo Condenser Tests.....31
3.4 Experimental Procedure for the Solo Condenser Tests.....32
4. ANALYSIS OF TEST DATA…….....35
4.1 Refrigerator Experiments……. 35
4.1.1 Design of Experimental Matrix and Effective Parameter Analysis.....35
4.2 Solo Condenser Experiments…….....39
4.2.1 General……. 39

4.2.2 Method of Calculation…….....39
4.2.2.1 Calculation of Heat Transfer Rates….....39
4.2.2.2 Calculation of Inside Convective Heat Transfer Coefficients.....40
4.2.2.3 Calculation of Outside Convective Heat Transfer Coefficients.....42
4.2.2.4 Calculation of Overall Heat Transfer Coefficients….....46
4.3 Second Stage Refrigerator Experiments.....47
4.3.1 Systematic of the Experimentss…….....47
5. RESULTS AND DISCUSSION…….....49
5.1 Results.....49
5.1.1 Refrigerator Tests Statistic Minitab Software Results.....53
5.1.2 Solo Condenser Results…….....57
5.1.2.1 Heat Transfer Rate Calculations…….....58
5.1.2.2 Inside Convective Heat Transfer Coefficient Calculations…….....59
5.1.2.3 Outside Convective Heat Transfer Coefficient Calculations….....59
5.1.2.4 *UA* and Overall Heat Transfer Coefficient Results…….....60
5.1.3 Second Stage Refrigerator Tests Results…….....61
5.2 Discussion……..…….....62
6. CONCLUSION …….....65
6.1 Conclusions 65
6.2 Recommendations for Future Work ….....66
REFERENCES 68
APPENDICES……..……70
APPENDIX A. Climatic Test Chamber and Power Analyzer Calibration Reports...70
APPENDIX B. Sample Solo Condenser Performance Calculations…….……74
APPENDIX C. Sample Condensation Line Drawn On *P-h* Diagram…….…….....82
APPENDIX D. Isobutane Physical Properties……..…….....83

LIST OF TABLES

Table 3.1: Geometric Parameters of the Tested Condensers…….……23

Table 3.2: Experiment Matrix…….…….…….……..…23

Table 3.3: Household Refrigerating Appliances Categories [12].....……..…25

Table 3.4: *M* and *N* Values for Household Refrigerating Appliances [12]…..…..…26

Table 3.5: Value of the Correction Factors [12]…….…….…….……..…27

Table 3.6: Energy Efficiency Level of Household Refrigerating Appliances…..…27

Table 3.7: Experimentally Investigated Refrigerating Appliance Energy Consumption Limits……...28

Table 3.8: Energy Measurement Tests Minimum Required Storage Temperatures in Different Compartments [13, 14]…..…….....29

Table 4.1: DOE Matrix Results….....36

Table 4.2: Determined Tube Lengths of Each Region…….....43

Table 4.3: Dimensions and Area Details of the Original and Shortened Tube Condensers.....47

Table 5.1: Subset of the Experimental Matrix for the Effects of Condenser Inclination…….…….....56

Table 5.2: Experimentally Measured Mass Flow Rate and Temperature Results ...58

Table 5.3: Heat Transfer Rate Results…….…….....58

Table 5.4: Inside Convective Heat Transfer Coefficient Results…….....59

Table 5.5: Outside Convective Heat Transfer Coefficient Results.....60

Table 5.6: *UA* Results 60

Table 5.7: Overall Heat Transfer Coefficient Results.....61

Table 5.8: Final Control Experiments Results……..….....61

Table 5.9: Total Overall Heat Transfer Coefficient Results…….…….....64

Table A.1: Sample Climatic Chamber Calibration Report.....70

Table A.2: Sample Calibration Report of Temperature Measurement Results.…....72

Table A.3: Sample Calibration Report of Voltage and Current Measurement Results.….....72

Table A.4: Sample Calibration Report of Power and AC Power Consumption Measurement Results.….....73

Table B.1: Condenser Geometric Properties…….....74

Table B.2: Length of Different Regions…….…...74

Table B.3: Condenser and Climatic Chamber Temperature Details…….....75

Table B.4: Desuperheating Region Refrigerant Properties……..….....75

Table B.5: Two Phase Region Refrigerant Properties…….....76

Table B.6: Subcooled Region Refrigerant Properties……...…….....77

Table B.7: Cavallini and Zecchin Correlation, Equivalent Reynolds Number Calculations…….78

Table B.8: Air Physical Properties…….…...78

Table B.9: Steel Tube and Wire Thermal Conductivities……..……...79

Table B.10: Airside Average Temperature Measurements ……..……..…...80

Table D.1: Isobutane Physical Propertiess……..….....83

LIST OF FIGURES

Figure 1.1: Domestic Type Experimentally Investigated Refrigerator…….....2

Figure 1.2: Energy and Energy Efficiency Studies Report about Turkish Electric Usage Ratios [1]…….……..2

Figure 1.3: Detailed House Electric Usage Distribution Ratios [1]……..……..3

Figure 1.4: Bundesverbant's Survey about Domestic Home Electricity Consumption Ratios [2]…….....4

Figure 1.5: Experimentally Investigated Condensers (a: Horizontal Tubes, b: Vertical Tubes, c: Shortened Horizontal Tubes).....5

Figure 2.1: Schlieren Technique Qualitative Sketches of the Boundary Layer around Heat Exchangers. [6]…….…….…….10

Figure 2.2: Illustration of Measured and Predicted Total Heat Transfer Rates Normalized by q_0 of The Tubes against Varied Geometrical Factors [6]……..…11

Figure 2.3: Schematic Representation of Wire-and-Tube Condenser, Elemental Unit of Condenser and Parameters of the Condensers [8]……..12

Figure 2.4: Comparison of the Results of the Modeling and the Experiments for the Wire-and-Tube Condenser [8]…….....13

Figure 2.5: Wire and Tube Type Heat Exchanger Geometrical Parameters [10]….14

Figure 2.6: Schematic of The Test Section and The Facility [10]……..…....…15

Figure 2.7: The Images of Distribution of Temperatures and Velocity of The Air Surrounding The Condenser Element by Natural Convection Conditions [11]…....16

Figure 3.1: Photographs of The Test Room from Outside (a) and Inside (b)……18

Figure 3.2: 3D Image of 4252 Arçelik Model Refrigerator and Condenser……..…19

Figure 2.3: Photographs of an M-package Thermocouple (a), a Pressure Transducer (b), a Thermocouple (c), an Air Velocity Transducer (d), Relative Humidity Transmitter (e)……..……..20

Figure 3.4: The Instrument Panel, Data Acquisition System and User Interface..…20

Figure 3.5: Condenser Inclination Change (Parallel and 1.5 ° Inclined) ……..…21

Figure 3.6: Condensers of Horizontal and Vertical Tubes……..……..……22

Figure 3.7: Prevention of Air Circulation and Temperature Measurement Points [13, 14]…….……..29

Figure 3.8: Temperature measurement points in fresh-food storage compartments [13, 14]……..…….……..…..30

Figure 3.9: Sample Loading Plan for Frozen Storage Compartment without Unventilated, Refrigerated Walls and Door Shelves [13, 14]……...…….30

Figure 3.10: Experimentally Investigated Refrigerator Loading Plan for the Frozen Storage Compartment …….……...…....31

Figure 3.11: Schematic Representation of the Experimental Setup for Solo Heat Exchangers…….....…….31

Figure 3.12: Schematic Representation of the Thermocouple and Pressure Transducer Locations in the Experimental Setup for Solo Heat Exchangers…….33

Figure 4.1: Main Effects Plot and Pareto Chart of DOE Analysis……..……..37

Figure 4.2: Main Effects Plot and Pareto Chart of DOE Analysis after Elimination of Non-effective Parameters…….……..38

Figure 4.3: Determination of the Tube Lengths Corresponding to the Desuperheating, Condensation, and Subcooled Regions……..……....…….43

Figure 4.4: Experimentally Determined Flow Characteristics Inside the Condenser and Surrounding Air Temperature Measurement Locations…….…….44

Figure 5.1: Freshfood Compartment Temperature Variation with Time……...50

Figure 5.2: Freshfood Average Temperature Variation with Time…….....50

Figure 5.3: Freezer Compartment Temperature Variation with Time……...51

Figure 5.4: Condenser Temperature Variation with Time……....…51

Figure 5.5: Detailed Condenser Temperature Variation with Time……..52

Figure 5.6: Power Consumption Variation with Time.....52

Figure 5.7: Energy Consumption in Time…….....53

Figure 5.8: Design of Experiment Results: Main Effects and Multiple Interactions Pie Chart……..54

Figure 5.9: Design of Experiment Results: Effective Parameters Pie Chart..……...54

Figure 5.10: Main Effects Plot for Energy Measurement Results ……..…..55

Figure 5.11: Interaction Plot for Energy Measurement Results with Condenser Inclination.....57

Figure 5.12: Heat Transfer Model for the Total Overall Heat Transfer Coefficient.63

Figure C.1: Sample Condensation Line Drawing on Isobutane P-H Diagram.....82

LIST OF SYMBOLS

A	Area	(m^2)
AE_c	Annual energy consumption	(kWh/year)
C_p	Specific heat of the refrigerant	(kJ/kgK)
D	Diameter	(m)
D_c	Characteristic length, $\frac{\frac{S_w}{S_t}d_0^2+d_w^2}{\frac{S_w}{S_t}d_0+d_w}$	
EEI	Energy Efficiency Index	
E_{24h}	Daily energy consumption of the product	(kWh/day)
g	Gravitational acceleration	(m/s^2)
Gr	Grashof Number, $g\beta(T_\infty - T_S)L^3 / v^2$	
h	Convective heat transfer coefficient	(W/m^2K)
k	Thermal conductivity	(W/mK)
L	Length	(m)
Nu	Nusselt Number, hL / k	
Q	Heat transfer rate	(W)
Pr	Prandtl Number, υ / α	
R	Thermal resistance	(m^2K/W)
Re	Reynolds number, $4\dot{m}_r/(\pi D_{t,in}\mu)$	
SAE_c	Standard Annual Energy Consumption	(kWh/year)
T	Temperature	(°C)
U	Overall Heat Transfer Coefficient	(W/m^2K)
V_{eq}	Equivalent volume of household refrigerating appliance	

Greek Letters

β	Isobaric thermal expansion coefficient	(K^{-1})
ρ	Density	(kg/m^3)
μ	Dynamic viscosity	(Pa.s)
η_f	Fin efficiency	

Subscripts

a	Air
amb	Ambient
cc	Cooling Compartment
f	Film
in	Inner
l	Liquid
L	Length
out	Outer
p	Pitch
r	Refrigerant
s	Spacing
sub	Subcooled Region
desup	Desuperheating Region
t	Tube
tot	Total
two	Two Phase Region
v	Vapor
w	Wire

CHAPTER 1

INTRODUCTION

1.1 Motivation

In recent years, with growing population and developing technology, energy shortage around the world is being observed. In order to eliminate the shortage, renewable energy sources are being investigated and the efficient use of energy has gained importance. Considerable effort is spent on the efficient use of energy and its sustainability. In order to survive in the global economy, companies must carry out production with high quantity and high quality. While increasing or maintaining the efficiency of the products, a small amount of cost reduction increases the profit and market share. As an example, for a producer of ten million refrigerators per year, decreasing the unit cost of the condenser by ten cents means a cost improvement potential of a million Euros per year.

In this study, refrigerator condensers are experimentally investigated for possible design improvements with the aim of reduced cost and energy consumption. The experimented household refrigerator is shown in Fig. 1.1.

Figure 1.1 Domestic type experimentally investigated refrigerator

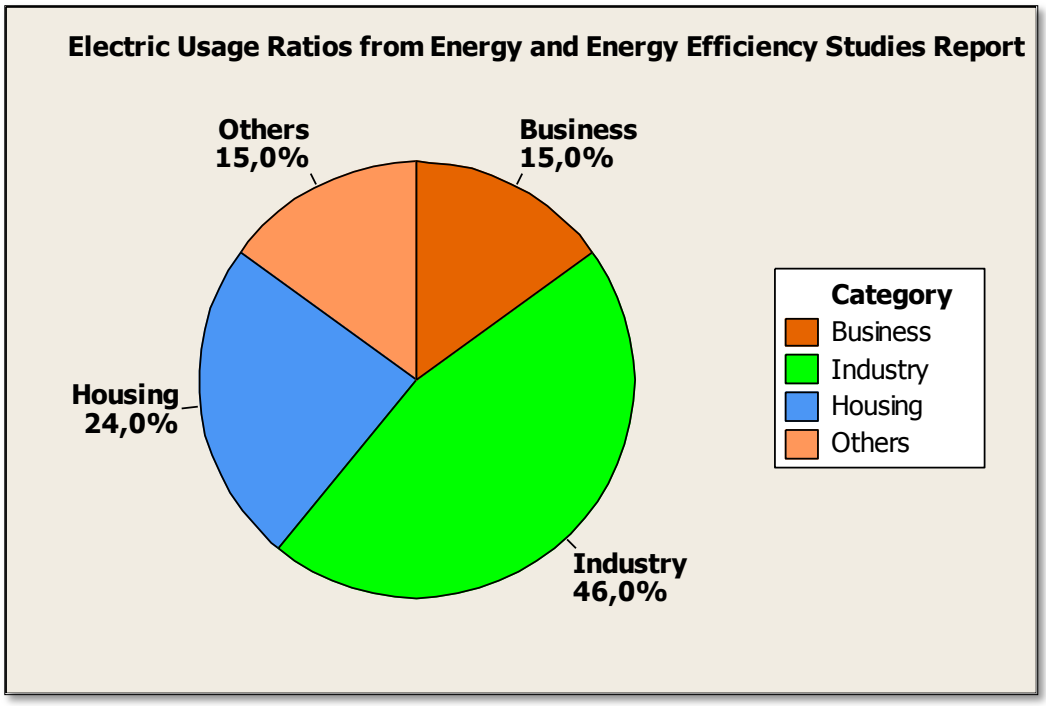

Figure 1.2 Energy and energy efficiency studies report about Turkish electric usage ratios [1]

One of the most widely used forms of energy is electrical energy throughout the world. As indicated in Fig. 1.2, according to the Energy and Energy Efficiency Studies published in July 2010, in Turkey, 24% of the electrical energy production is used in homes. [1]

According to the same report, household appliances are responsible of about 55% of residential electricity consumption. When TV and air conditioning are added, this value reaches 71%. A more detailed look at the group of household appliances (Fig. 1.3) indicates that the refrigerator and freezer play an important role with an electricity consumption of 31%.

The Bundesverband der Energie-und Wasserwirtschaft (BDEW) survey conducted in 2008; support this result by stating that coolers take a consumption share of 29% in domestic electricity usage [2]. Results of the survey are illustrated in Fig. 1.4.

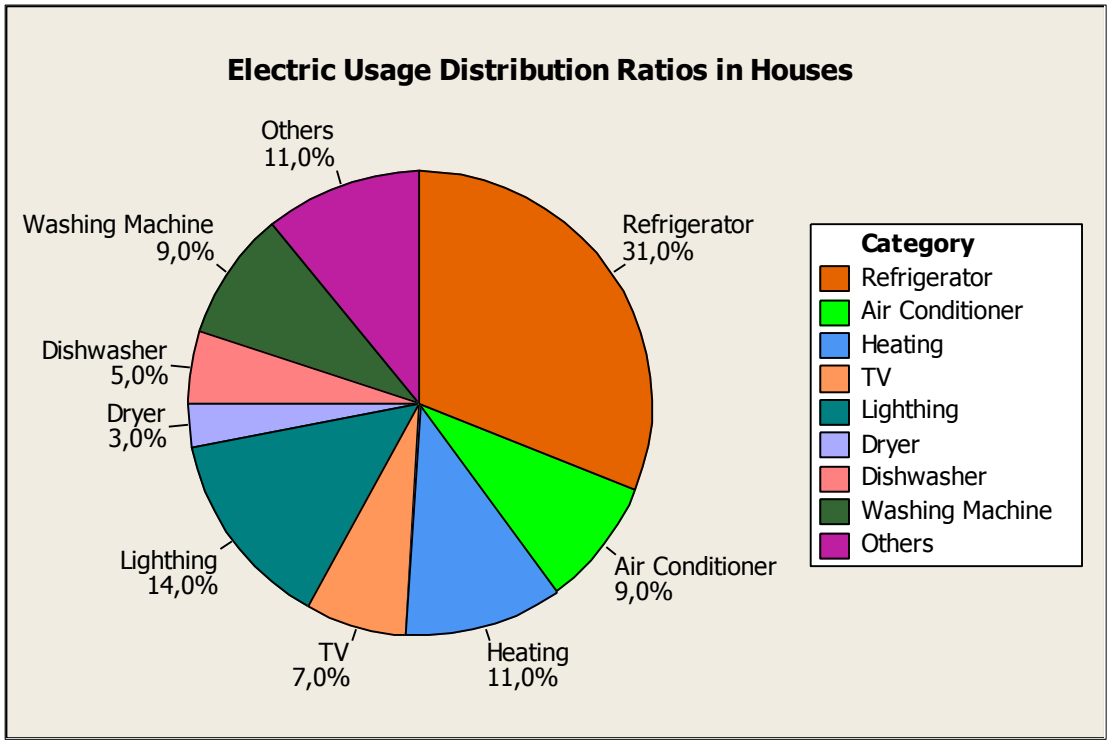

Figure 1.3 Detailed house electric usage distribution ratios [1]

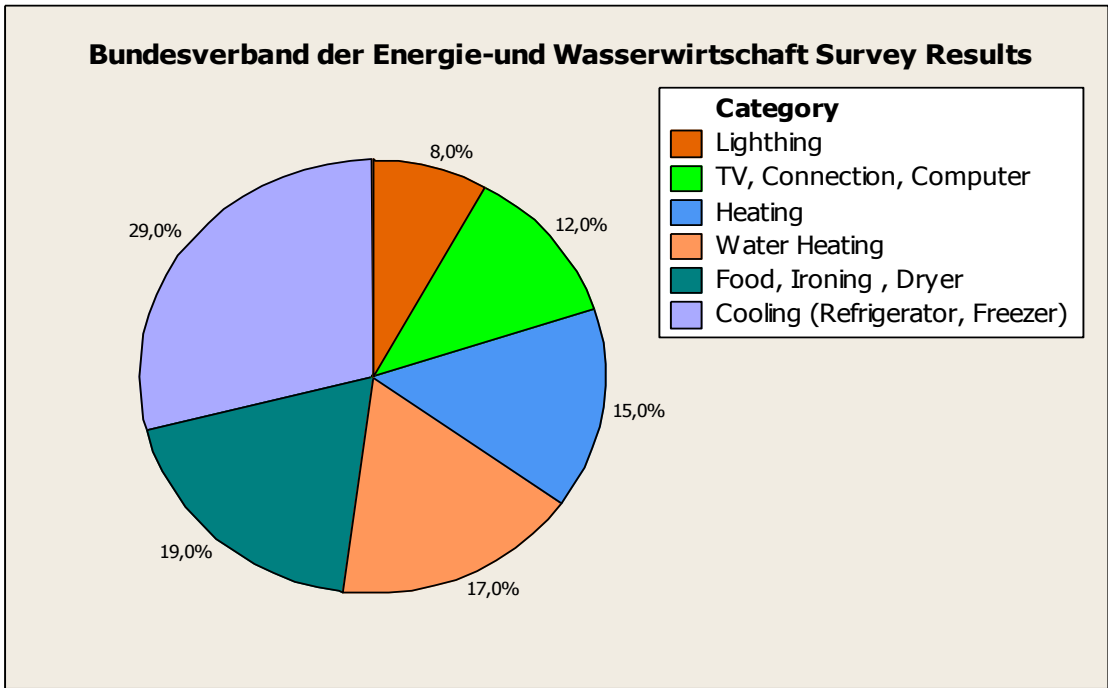

Figure 1.4 Bundesverbant's survey about domestic home electricity consumption ratios [2]

Refrigerator is usually the appliance that consumes the most energy in the household while household electricity consumption constitutes an important portion in the overall energy consumption. In order to obtain A++, A+++ and A+++ -%20 energy level products, the cooling cycle has to be improved. Energy efficiency index and their relation with energy levels are explained in chapter three. A wide variety of choices exist for making household refrigerators more efficient. So far, the energy saving performances of refrigerators can be improved by: a) Using high efficiency compressor, which has a direct impact on the coefficient of performance of the cooling system; b) Optimizing the match and control of the system by adopting advanced circulation; c) Improving the thermal insulation of refrigerators by thickening the insulation or using other advanced thermal insulation techniques; d) Optimizing the heat transfer of the evaporator and the condenser. However, these improvement techniques are limited by various design constraints and cost-ups. The refrigerator condenser is the main heat rejecting part of the cooling cycle. Heat is transferred from the refrigerant inside the condenser to medium outside. As a result of losing heat to the surroundings, the initially superheated refrigerant cools down to

saturation state and then condenses. Mainly, two types of condensers are used in the design of home appliances.

1. Natural circulation air-cooled condensers
2. Forced circulation air-cooled condensers

1.2 Air-Cooled Condensers

Air cooled condensers use air as the cooling medium. In the natural circulation, since the air circulation around the condenser is low, a large condensing section is required. The condensers could be made of copper, steel or aluminum tubing with attached fins to improve the air side heat transfer. In the cooling system, the refrigerant flows inside the tubes and air passes over the finned area of the condenser. Wire-and-tube type condensers consist of tubes and wires used as extended surfaces. The wires are spot welded to the tubing, on both sides perpendicularly. The wire-and-tube type condensers are generally mounted on the back side of the refrigerator. A few different designs also exist in which the condenser can be mounted on the top or bottom of the refrigerator. A typical wire-and-tube type condenser is shown in Figure 1.5.

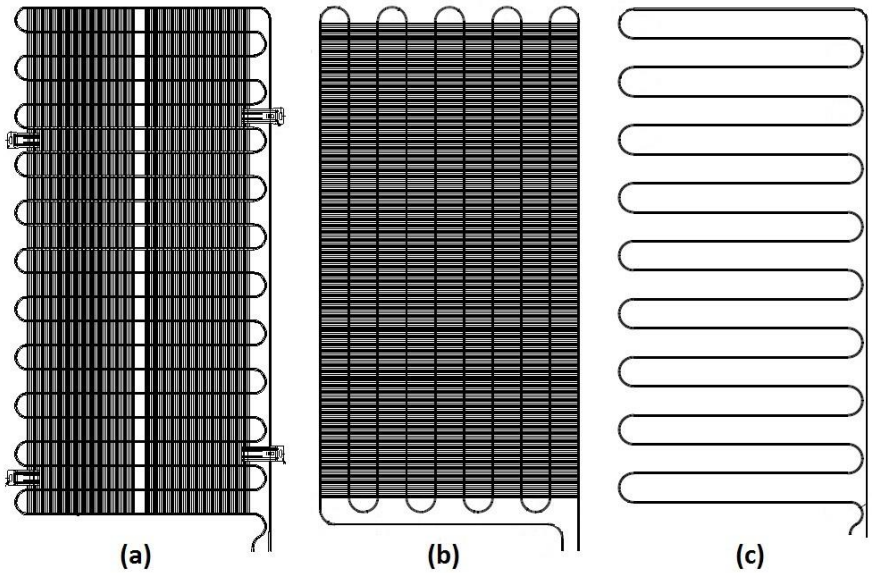

Figure 1.5 Experimentally investigated condensers (a: horizontal tubes, b: vertical tubes, c: shortened horizontal tubes)

1.3 Present Study

The main objective of this study is to test and evaluate different types of air-cooled, wire-and-tube type refrigerator condensers, in order to suggest possible performance and cost improvements.

For the experiments, two different experimental set-ups have been used. For the refrigerator performance tests, (the first and the third parts of the study), a climatic test chamber has been provided by Arçelik A.Ş. Refrigerator Plant in Eskişehir. For the solo condenser tests (the second part of the study), a heat exchanger characteristics measurement test room has been provided by the Fluid Mechanics Laboratories of Arçelik A.Ş. Central Research and Development Center in İstanbul. A review of the literature revealed that similar studies have been completed with hot water, R22 and R134a as the working fluid. The refrigerant isobutane (R600a), however, has not been investigated before. In all three parts of the present study isobutane has been used to determine the condenser performances.

As a result of forty refrigerator performance tests, and twenty four condenser experiments a vast amount of data have been collected. The experimental measurements have been performed in around 6 months. Utilizing the data, refrigerator performance comparisons, heat transfer rates, inside and outside heat transfer coefficients, and overall heat transfer coefficients have been determined.

1.4 Thesis Outline

The following chapter presents a detailed literature review. Chapter 3 focuses on the experimental setups and procedures, and explains the measurement methods and techniques. The effects of different parameters on energy consumption, the data reduction methods, and correlations to determine the overall heat transfer coefficients are given in Chapter 4. The results of the experiments are presented and discussed in Chapter 5. The summary, conclusions and future work are stated in Chapter 6.

CHAPTER 2

LITERATURE REVIEW

Air-cooled condensers are widely used in household refrigeration appliances. However, despite the widespread use of these heat exchangers, only a few detailed studies which deal with heat transfer performance are available in the literature. In this chapter, experimental studies on about wire-and-tube type condensers have been summarized. The experiments indicated that the condensers capacity and cost could be improved by changing the condenser tube and wire diameters.

In 1957, Witzell and Fontaine [3] performed an experimental study and tried to find out heat transfer characteristics of wire-and-tube type condensers. They have tested the condensers with their tubes in horizontal position. Their aim was to investigate the effect of the wire-and-tube geometry on heat exchanger performance. They have defined the characteristic dimension of the condenser for the evaluation of the Nusselt and Grashof numbers as

$$D_c = \frac{A_{t,out} D_{t,out} + A_w D_w}{A_{t,out} + A_w} \tag{2.1}$$

where $A_{t,out}$: Tube outer surface area (m^2)

A_w : Total wire area (m^2)

$D_{t,out}$: Tube outer diameter (m)

D_w : Wire diameter (m)

Reduction of the experimental data resulted in the correlation expressed by

$$Nu = 0.4724 Gr^{0.2215} \tag{2.2}$$

There are some drawbacks of the study of Witzell and Fontaine [3]. They did not measure the surface temperature of the condensers, and did not use wire spacing (S_w) or tube spacing (S_t) in the definition of characteristic length.

In 1959, Witzell *et al*. [4] realized that the data obtained in the previous studies were questionable. They improved the techniques for measuring the temperature and the mass flow rates. They have used a cell which was designed to provide the necessary control of the environment. The cell allowed the measurements to be more precise. The wall and ambient temperature measurements were utilized to determine the existence of a steady state condition.

The experimental results for the vertical tests yielded the correlation

$$Nu = 0.034Gr^{0.925} \tag{2.3}$$

which implied that heat exchanger was acting like a flat plate. The characteristic dimension for this study was given as

$$D_c = \left[\frac{A_{t,out}+A_w}{\frac{A_{t,out}}{D_{t,out}^{0.25}}+\frac{\eta_f A_w}{D_w^{0.25}}}\right]^4 \tag{2.4}$$

where η_f is the fin efficiency, and it was assumed that $h = CD^{-1/4}$ for the cylinders in natural convection in the same medium and temperature.

For the effect of boundary layer interference of the wires, it is necessary to modify the correlations using a geometrical factor. Since the tube plays a small part in the total heat transfer from the condenser, the geometry factor should be dependent on the wire configuration. Witzell et *al.* [4] improved the correlation for the Nusselt number as

$$Nu = 0.905Gr^{0.176}\left(\frac{S_w-D_w}{S_w}\right)^{0.5} \tag{2.5}$$

where S_w is the wire spacing.

In 1995, Hoke *et al*. [5] investigated the air side convective heat transfer from wire-on-tube heat exchangers in forced flow. They have constructed an induced flow wind tunnel to test the wire-and-tube heat exchanger in a well-defined flow field. An electronically controlled bath supplied constant temperature hot water to the exchanger. The mass flow rate during the experiments was adjusted by changing the supply pressure. Water was circulated through the condensers. In order to separate the convective heat transfer from the total, the radiative heat transfer rate was also evaluated considering that all of the surfaces are diffuse and gray.

Hoke *et al*. [5] investigated the air-side convection heat transfer for seven different forced type condensers, and suggested correlations for the Nusselt number. Their experiments showed that wire-and-tube heat exchangers which are cooled by forced convection should be designed with certain a angle of attack. The convective heat transfer from the wire-and-tube heat exchangers increases with increasing air velocities and/or angle of attack in the forced convection regime.

In 1997, Tagliafico and Tanda [6] experimentally studied the effects of radiation and natural convection between condenser outer surface and the surrounding air. In this study, the exchanger was vertically oriented without confining walls. Heat exchangers were coated with a low emissivity ($\varepsilon \approx 0{,}35$) paint to minimize the radiant heat transfer. The radiation part was calculated analytically using diffuse, gray body assumptions. For the free-convection part, a semi-empirical correlation was developed by changing the condenser tube and wire geometry. The water mass flow rate was measured by a turbine flow meter and temperature difference across the wires was measured by infrared thermography. The fin efficiency was defined assuming uniform heat transfer coefficient along the wire surfaces as

$$\eta_w = \frac{T_w - T_\infty}{T_t - T_\infty} \tag{2.6}$$

They have also calculated the fin efficiency using one dimensional fin analysis as

$$\eta_f = \frac{\tanh\left(mS_t/_2\right)}{m\frac{S_t}{2}} \tag{2.7}$$

$$m = \sqrt{\frac{4h_o}{k_w d_w}} \tag{2.8}$$

where S_t : Tube spacing (m)

k_w : Thermal conductivity of wire material (W/mK)

D_w : Wire diameter (m)

h_o : Outside convective heat transfer coefficient (W/m^2K)

Experiments showed that fin efficiencies calculated from two different methods differed only by 4 percent, hence, the one-dimensional fin model assumption for the evaluation of h_o was stated to be suitable.

Tagliafico and Tanda [6] have also studied flow visualization. For this purpose, color Schlieren technique was used. This technique is based on the variation of refraction index of a transparent medium with density. At the end, in an artificial way, a colored picture is obtained around the exchangers. It was stated that the boundary layer is laminar within 20 cm of the leading edge after which intermittent flow disturbances become important. On the upper side, fully turbulent flow observed (See Figure 2.1).

For all of the varied parameters they created comparison tables for the measured and predicted results (See Figure 2.2).

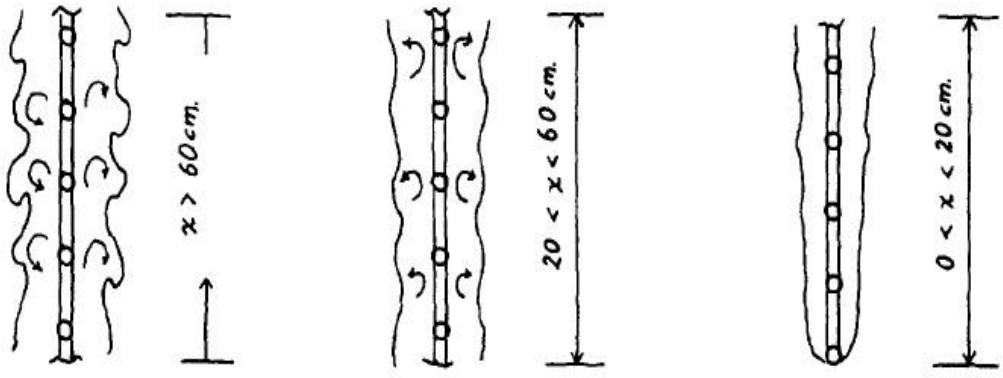

Figure 2.1 Schlieren technique qualitative sketches of the boundary layer around heat exchangers [6].

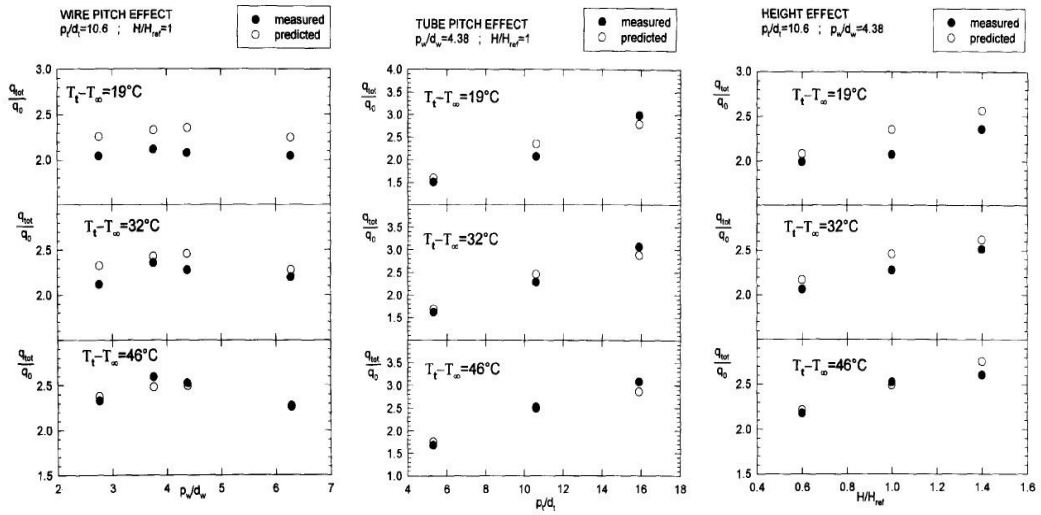

Figure 2.2 Illustration of measured and predicted total heat transfer rates normalized by q_0 of the tubes against varied geometrical factors [6].

In [6], the effect of the main geometrical and operating parameters on heat transfer performance was separately investigated. In the experiments, hot water was used to simulate the refrigerant flow inside the exchangers. The temperature difference between tube wall and the surrounding air ranged from 15 to 50°C, which is high for household refrigeration systems.

In 1999, Okutucu [7] has constructed a test setup for the experimental evaluation of refrigerator condensers. A wire-and-tube type condenser was tested in order to determine its performance characteristics. Hot water was used inside the tube of the wire-and-tube type condenser. In the experiments the following parameters were changed: the mass flow rate, the inlet temperature of water, the spacing between the refrigerator and the condenser, the spacing between the condenser and the room wall. Finally, the total capacity of the condenser, the overall heat transfer coefficient, and the outside equivalent heat transfer coefficient including convective and radiative components were determined.

In 2002, Bansal and Chin [8], created a model to optimize wire-and-tube type condensers. They developed simulations using finite element techniques and conductance approach. The condenser capacities were analyzed by changing the distance between the condenser tubes and the wire diameter. The geometry of the condenser they used is illustrated in Figure 2.3.

In order to validate the model they performed experiments on real refrigerators, and measured the temperature, pressure, mass flow rate and the power consumption of the refrigerator. In terms of the condenser capacity for different saturation temperatures they showed that the results of the model agree with the experimental results to within ±10% as shown in Figure 2.4

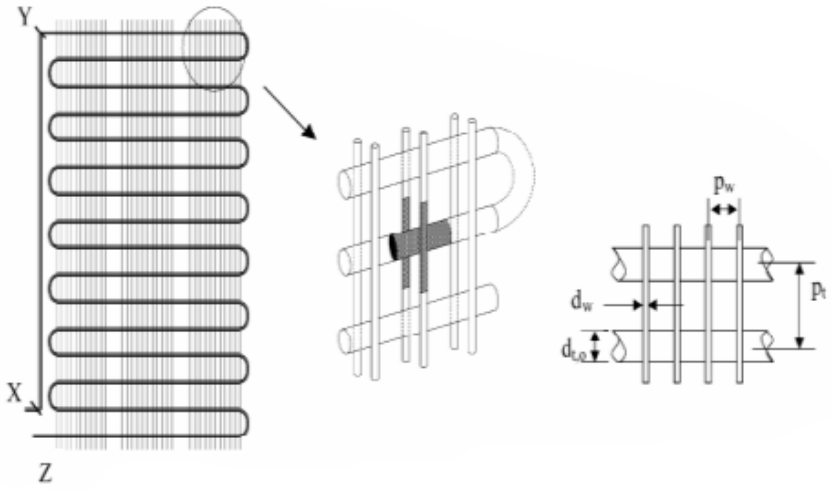

Figure 2.3 Schematic representation of wire-and-tube condenser, elemental unit of condenser and parameters of the condensers [8].

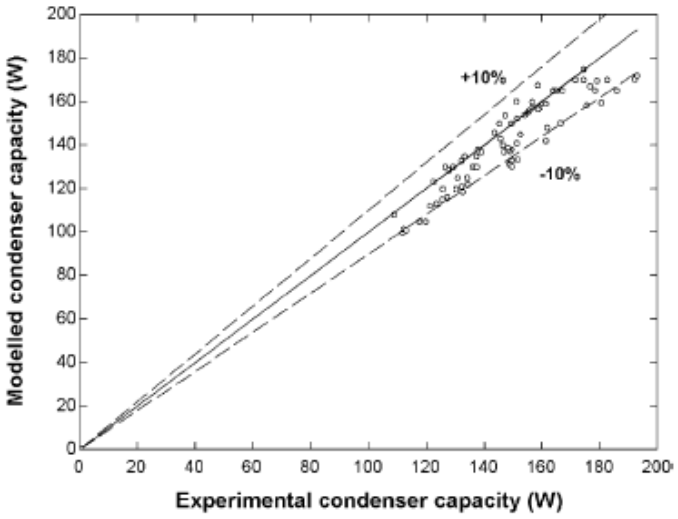

Figure 2.4 Comparison of the results of the modeling and the experiments for the wire-and-tube condenser [8].

In the conclusion part of Bansal and Chin's study [8], it was stated that the condenser capacity increased with increasing wire diameter and the number of rows, but their optimization factor (f_o) showed the opposite. That means the optimization process revealed two improved designs, one optimized for the condenser capacity and the other optimized for decreased condenser weight.

In 2002, Dirgin [9] experimentally investigated a variety of air-cooled wire-and tube type condensers in order to determine their performance characteristics. A similar setup to that of Okutucu [7] was used for different condenser geometries. Hot water was used inside the wire-and-tube type refrigerator condenser. The number of wires, the wire spacing and therefore the tube and wire area were the experimental variables. The capacity of the condenser, the overall heat transfer coefficient and the outside equivalent heat transfer coefficient were determined. The radiative calculations were performed theoretically.

Using the calculated outside heat transfer coefficients, the variation of Nusselt number with respect to Grashoff number was investigated.

In Dirgin [9], all three condensers had the same number of tube passes and the same spacing, but they differed by the number of wires and the wire spacing. It was observed that placing the wires to one side of the condenser with lower wire

spacing had more positive effect than placing the wires on both sides of the condenser with greater wire spacing using the same number of wires.

In 2008, Melo *et al*. [10] studied natural draft wire-and-tube condensers. In their study, a dimensionless correlation to estimate the combined (radiation and natural convection) heat transfer coefficient between the external surfaces of the wire-and-tube condensers and the surrounding air was developed. The correlation took into account seventy two different combinations of the tube outer diameter (d_t), the number of tube rows (N_t), the number of wire pairs (N_w), the wire pitches (p_w) and the tube pitches (p_t) (See Figure 2.5).

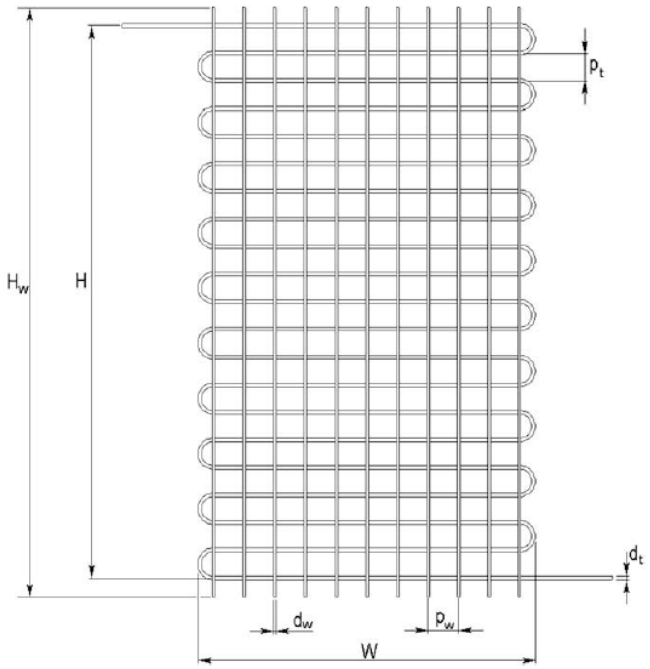

Figure 2.5 Wire and tube type heat exchanger geometrical parameters [10].

In the experiments, hot water was used inside the condenser, and the total heat rejection rate was calculated from the water flow rate measurements and the temperature difference from the inlet to the exit through the exchanger. The radiation heat transfer rate was calculated by a simplified process and subtracted from the total heat transfer rate to obtain the convective part of the heat transfer.

The tests were conducted inside a temperature and humidity controlled chamber constructed according to ISO 15502 (2005) standards. The test room was maintained at 32°C during the experiments. The test section is shown in Figure 2.6.

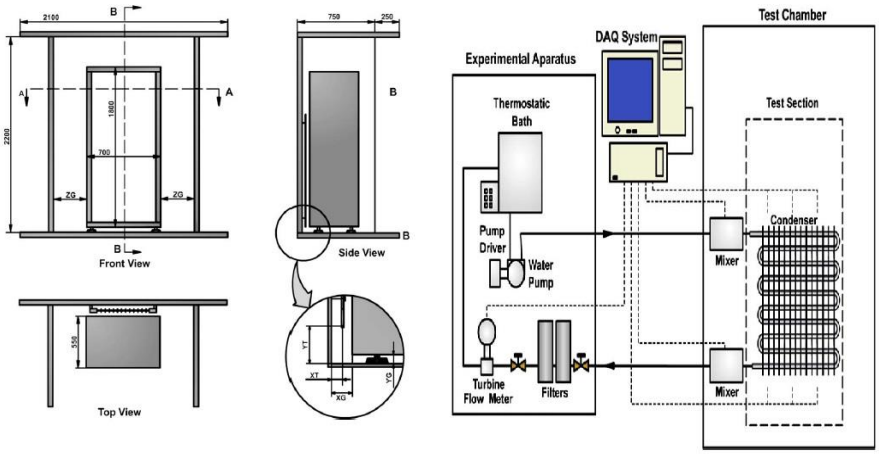

Figure 2.6 Schematic of the test section and the facility [10].

The Buckingham-Pi theorem was used to derive dimensionless parameters for the working temperatures and the heat exchanger geometry variations. Although the correlation factor gives 90% precision, the average temperature difference between the air and the water at the inlet of the condenser was kept at around 30°C which was not realistic.

In 2012, Hofmanas and Paukstaitis [11] numerically investigated external heat transfer of wire-and-tube condensers. By using the ANSYS CFX program they simulated 1/5 of the condenser, they have chosen the air temperature in the condenser space as 25°C and the temperature of the condenser tube as 40°C and adopted the boundary conditions.

Thermo visional images from numerical simulation of developed model were also obtained as shown in Figure 2.7. It was observed that the local air speed by natural convection was only about 0.05 m/s. In order increase the local air speed, a fan motor was used and mixed convection was created. It was stated that naturally rising air gets warmer and reduces the efficiency of the heat transfer, and mixed convection provides an improvement in the performance of the refrigerators.

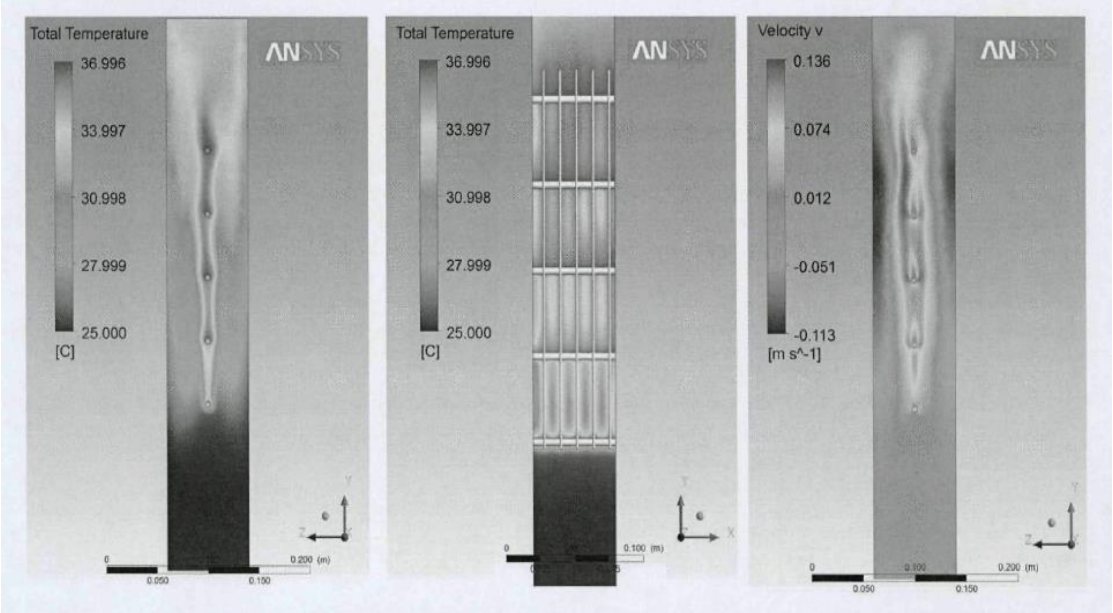

Figure 2.7 The images of distribution of temperatures and velocity of the air surrounding the condenser element by natural convection conditions [11].

In the refrigerator industry 4.76 mm outer diameter steel tubes are well known, but recently 4 mm outer diameter steel tubes has started to take part in the market. As can be observed from the literature survey, several studies have been performed on condensers and condenser optimization. However, none of them covered the effect of tube dimension, as well as condenser inclination on the condenser performance. In addition, no correlations have been suggested in the literature for the heat transfer coefficient for vertical tube orientation. By handling different tube outer diameters, condenser inclinations, and tube orientations, the present work focuses on what is missing in the literature.

CHAPTER 3

EXPERIMENTAL PROCEDURE

3.1 Experimental Setup for the Refrigerator Tests

A 4252 model Arçelik static type A+ energy level refrigerator was prepared for the energy performance tests and put into a test chamber provided by Arçelik A.Ş. Refrigerator Plant in Eskişehir. Thermocouples, air velocity transducers, pressure transducers and relative humidity sensors were located in accordance with IEC 62552 standards, which contain characteristics and test methods for household refrigerating appliances. By an instrument panel, the temperature and relative humidity of the test chamber were set. The measured temperature and power consumption data were recorded by a data acquisition system and a PC. Below, a detailed description of the experimental setup is provided.

In order to place the refrigerator and make the necessary tests, a climatic test chamber is used. The chamber is constructed according to ISO 15502 standards in terms of temperature, air velocity, relative humidity, surface radiative properties such as the emissivity, and geometric factors such as separators and dimensions. There are six stations in one chamber. A photograph from climatic test chamber is shown in Figure 3.1.

(a) (b)

Figure 3.1 Photographs of the test room from outside (a) and inside (b).

The temperature of the climatic test chamber can be set between 0°C to 65°C with 1°C control steps. At steady state, the temperature allowance is 0.5°C. The relative Humidity (RH) of the climatic test room can be changed between 30% and 95% by the control unit. The steady state relative humidity allowance is 3-5%. Sample pages of the climatic room calibration report and power analysis report are shared in Appendix A.

In order to balance the atmospheric pressure inside and outside the test chamber, there is a damper at the backside of the chamber. The chamber is cooled and heated by homogenously distributed air circulation. For heating, an electrical heater is used and for cooling there is an R-22 refrigerant cooling system. Air velocity in the test chamber is a maximum of 0.2 m/s in every direction. Data acquisition system uses multimeters to record the data. The test chambers are calibrated twice a year.

In order to reach A++ energy level for an Arçelik 4252 static type refrigerator of 450 liter capacity and 183x70x63 cm outer dimensions has been selected for the experiments, and is shown in Figure 3.2. The refrigerator has the freezer compartment at the top and the fresh food compartment at the bottom. The condenser is placed on the back side of the refrigerator as usual.

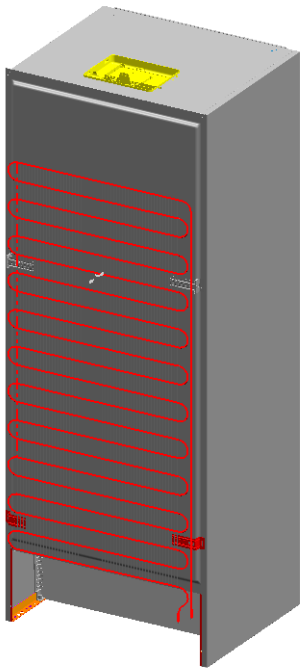

Figure 3.2 3D Image of 4252 model Arçelik refrigerator and condenser.

Ten T type thermocouples (N/N-24-TT IEC) have been used to measure the temperatures of specified locations on the refrigerator. In the energy consumption tests, eight measurement packages have been used in the freezer compartment and four thermocouples have been placed in the fresh food compartment. Additionally, the inlet and the outlet temperatures of the condenser have been measured by two thermocouples. In order to determine the phase of the refrigerant inside of the tubes, at the inlet and exit of the heat exchanger, two pressure transducers have been used. An air velocity transducer has been used to measure the air velocity in the test room, and a relative humidity transmitter measured the relative humidity in the room. Photographs of thermocouples, measurement packages, air velocity transducer, pressure transducer, and relative humidity transmitter are given in Figure 3.3.

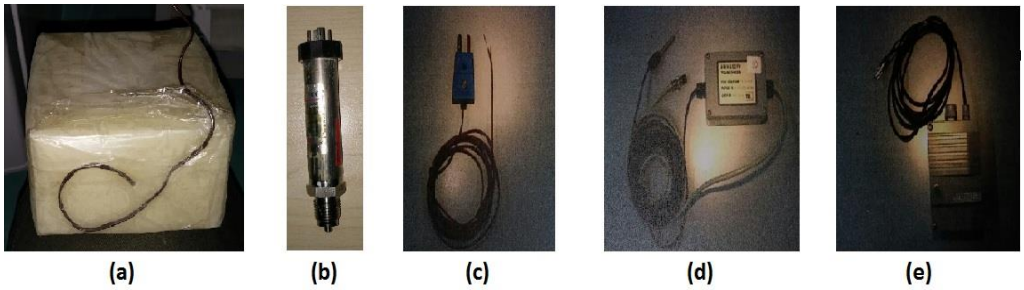

Figure 3.3 Photographs of an M-package thermocouple (a), a pressure transducer (b), a thermocouple (c), an air velocity transducer (d), relative humidity transmitter (e).

Figure 3.4 The instrument panel, data acquisition system and user interface.

The user interface displays both the set and measured temperature and relative humidity of the test room. The temperature measurements are performed continuously and displayed and stored using a PC. In Figure 3.4, a photograph of the data acquisition system and the user interface is given.

3.2 Experimental Procedure for the Refrigerator Tests

In the performance analysis of different types of refrigerator condensers, the following experimental parameters have been investigated:

- The condenser tube outer diameter,
- The condenser inclination,
- Orientation of the tubes (vertical or horizontal).
- Amount of refrigerant

In the refrigerator industry 4.76 mm outer diameter steel tubes are well known, but recently 4 mm outer diameter steel tubes has started to take part in the market. In the past, several studies have been performed on condensers and condenser optimization, but none of them covered the effect of tube dimension on condenser performance.

The condenser inclination could affect the performance of the appliance. In the experimental study, parallel or inclined condensers have been investigated (See Figure 3.5).

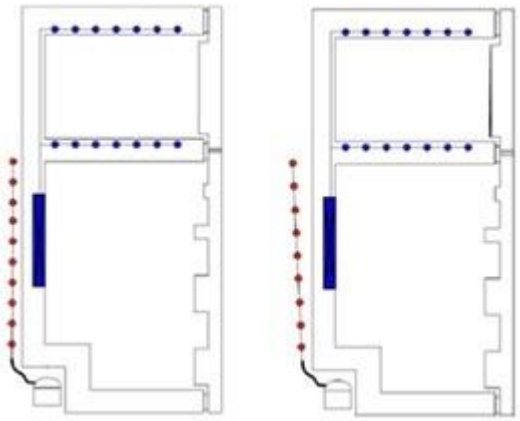

Parallel Condenser without Inclination

Inclined Condenser

Figure 3.5 Condenser inclination change (parallel and 1.5° inclined)

The orientation of the condenser tubes is also selected as an important design parameter in the study. In Arçelik products, condensers of both horizontal and vertical tubes are used as illustrated in Figure 3.6.

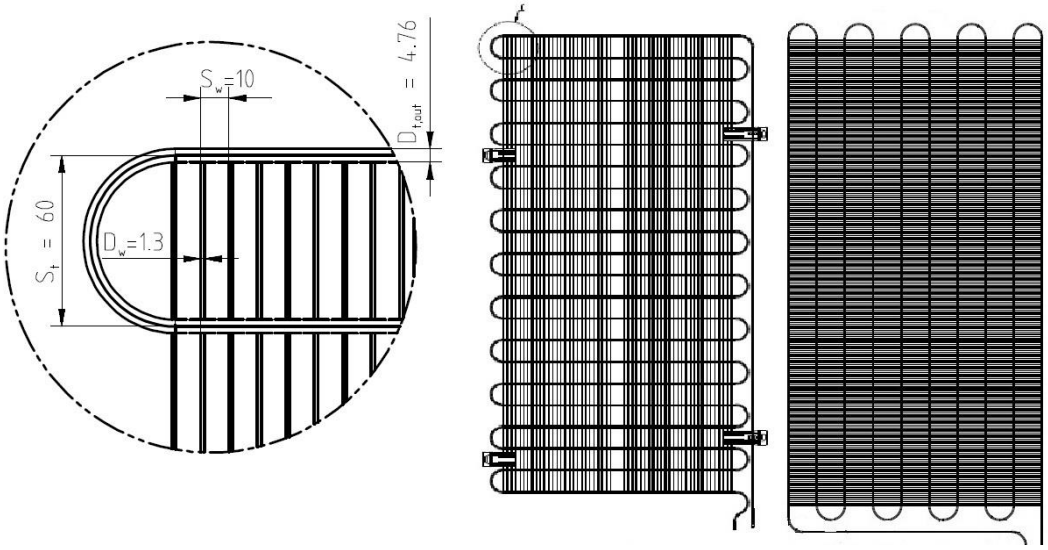

Dimension Details Horizontal Orientation Vertical Orientation

Figure 3.6 Condensers of horizontal and vertical tubes.

The tube inner and outer areas, the total wire area, and the total outer area of the condenser can be calculated via equations 3.1-3.4, respectively. The results of the geometric calculations are given in Table 3.1.

$$A_{t,in} = \pi D_{t,in} L_t \tag{3.1}$$

$$A_{t,out} = \pi D_{t,out} (L_t - n_t n_w D_w) \tag{3.2}$$

$$A_w = \pi n_w D_w L_w \tag{3.3}$$

$$A_o = A_{t,out} + A_w \tag{3.4}$$

Table 3.1. Geometric parameters of the tested condensers.

	Horizontal		Vertical	
	4mm	**4.76mm**	**4mm**	**4.76mm**
Tube Outer Diameter D_{to} (mm)	4	4.76	4	4.76
Tube Inner Diameter D_{ti} (mm)	3	3.36	3	3.36
Tube Spacing S_t (mm)	60	60	75	75
Number of Passes, n_t	22	22	10	10
Total Tube Length L_t (mm)	15850	15850	13460	13460
Wire Diameter D_w (mm)	1.3	1.3	1.3	1.3
Wire Length L_w (mm)	1260	1260	630	630
Number of Wires n_w	108	108	232	232
Wire Spacing S_w (mm)	10	10	10	10
Wire Perimeter P_w (mm)	4.084	4.084	4.084	4.084
Width of the Condenser W (mm)	630	630	630	630
Height of Condenser H (mm)	1260	1260	1230	1230
Total Tube Inner Area A_{ti} (m^2)	0.15	0.167	0.127	0.142
Total Tube Outer Area A_{to} (m^2)	0.16	0.19	0.131	0.156
Total Wire Area A_w (m^2)	0.555	0.555	0.597	0.597
Total Outer Area Ao (m2)	0.716	0.746	0.728	0.753

For the evaluation of multiple interactions of the four different parameters mentioned above, an experimental matrix has been created as shown in Table 3.2. The experimental procedure started with a gas charge optimization test for every interaction. After determining the optimized gas charges, the energy measurement tests have been completed for each interaction.

Table 3.2 Experimental Matrix

Tube Outer Diameter (mm)	Condenser Inclination (1.5°)	Tube Orientation	Amount of Refrigerant (gr)
4	Yes	Horizontal	48
4	Yes	Horizontal	56
4	No	Horizontal	48
4	No	Horizontal	56
4.76	Yes	Horizontal	50
4.76	Yes	Horizontal	57
4.76	No	Horizontal	50
4.76	No	Horizontal	57
4	Yes	Vertical	48
4	Yes	Vertical	56
4	No	Vertical	48
4	No	Vertical	56
4.76	Yes	Vertical	50
4.76	Yes	Vertical	57
4.76	No	Vertical	50
4.76	No	Vertical	57

3.2.1 Optimization Test for the Amount of Refrigerant

In the gas charge optimization tests, refrigerators with different design parameters are placed in 43°C, 55% humidity test chamber to determine the optimized gas charge initially. In order to perform the gas charge test, a special product is made during the trial production. At the inlet and exit of the refrigerator evaporators, thermocouples are placed. During the tests, the refrigerator compressors are run at 100% capacity. The minimization of the temperature difference between the inlet and the exit of evaporator is aimed. When the steady state conditions are reached, additional two or three grams of refrigerant is added to the system. This procedure starts with a low refrigerant charge, and continues until zero difference between the inlet and exit temperatures of the evaporators is achieved. Then, from the power and temperature graphs, two different optimized gas charges for minimal energy consumptions are determined.

3.2.2 Refrigerator Energy Efficiency Index Calculation

In the calculation of the Energy Efficiency Index (*EEI*) of a household refrigerating appliance, its annual energy consumption is compared to its standard annual energy consumption [12]. The Energy Efficiency Index (*EEI*) is calculated using the following formula.

$$EEI = \frac{AE_c}{SAE_c} 100 \tag{3.5}$$

where

AE_C : Annual energy consumption of the household refrigerating appliance,

SAE_C : Standard annual energy consumption of the household refrigerating appliance.

The annual energy consumption (AE_C) is calculated in terms of kWh/year;

$$AE_c = E_{24h} 365 \tag{3.6}$$

where

E_{24h} : Daily energy consumption of the household refrigerating appliance (kWh/24h).

The standard annual energy consumption (SAE_C) is calculated in kWh/year as

$$SAE_c = V_{eq}M + N + CH \tag{3.7}$$

where

CH: Chiller compartment bonus of 50 kWh/year added for appliances with storage volume of at least 15 litres.

V_{eq} : the equivalent volume of the household refrigerating appliance.

M and *N* values are selected according to the household product categories given in Table 3.3.

Table 3.3 Household Refrigerating Appliance Categories [12]

Category	**Designation**
1	Refrigerator with one or more fresh-food storage compartments
2	Refrigerator-cellar, Cellar and Wine storage appliances
3	Refrigerator-chiller and Refrigerator with a 0-star compartment
4	Refrigerator with a one-star compartment
5	Refrigerator with a two-star compartment
6	Refrigerator with a three-star compartment
7	Refrigerator-freezer
8	Upright freezer
9	Chest freezer

The investigated household product belongs to the 7th category, which is refrigerator- freezer with four star freezer compartment. *M* and *N* values for all categories are given in Table 3.4 [12].

Table 3.4 *M* and *N* Values for Household Refrigerating Appliances [12]

Category	***M***	***N***
1	0.233	245
2	0.233	245
3	0.233	245
4	0.643	191
5	0.450	245
6	0.777	303
7	0.777	303
8	0.539	315
9	0.472	286

Equivalent volume is calculated with the following formula.

$$V_{eq} = \left[\sum_{c=0}^{c=n} V_c \left(\frac{25-T_c}{20}\right) FF_c\right] CC.BI \quad (3.8)$$

where

n: Number of compartments

V_c: The storage volume of the compartments

T_c: Nominal temperature of the compartments as will be given in Table 3.8

FF_c, *CC* and *BI* are the correction factors given in Table 3.5.

Table 3.5 Correction Factors

Correction factor	Value	Conditions
FF (frost-free)	1.2	For frost-free frozen-food storage compartments
	1	Otherwise
CC (climate class)	1.2	For T class (tropical) appliances
	1.1	For ST class (subtropical) appliances
	1	Otherwise
BI (built-in)	1.2	For built-in appliances under 58 cm in width
	1	Otherwise

The energy efficiency level of the household appliance is determined based on its Energy Efficiency Index (*EEI*) given by Equation 3.5. The energy efficiency levels of household refrigerating appliances are stated in Table 3.6.

Table 3.6 Energy Efficiency Level of Household Refrigerating Appliances

Energy efficiency class	Energy Efficiency Index
A+++ (most efficient)	$EEI < 22$
A++	$22 \leq EEI < 33$
A+	$33 \leq EEI < 42$
A	$42 \leq EEI < 55$
B	$55 \leq EEI < 75$
C	$75 \leq EEI < 95$
D	$95 \leq EEI < 110$
E	$110 \leq EEI < 125$
F	$125 \leq EEI < 150$
G (least efficient)	$EEI \geq 150$

The experimentally investigated refrigerator is SN-T climate class, static type (not frost free), and freestanding (not built in) product. Hence, the respective FF_c, *CC* and *BI* correction factors are 1, 1.2 and 1. Storage volume of each compartment, equivalent volume, standard annual energy consumption and energy efficiency index are given in Table 3.7.

Table 3.7 Experimentally Investigated Refrigerating Appliance Energy Consumption Limits

Freshfood Compartment Storage Volume $\boldsymbol{V_{ff}}$ (lt)	340
Freezer Compartment Storage Volume $\boldsymbol{V_{frz}}$ (lt)	106
Category of Product	7
Equivalent Volume $\boldsymbol{V_{eq}}$ (lt)	681.48
Standard Annual Energy Consumption $\boldsymbol{SAE_c}$ (kWh/year)	832.51
A+ Energy Level (42 Index) Energy Consumption Limit (kWh/year)	349.65
A+ Energy Level (42 Index) Energy Consumption Limit (kWh/day)	0.958
A++ Energy Level (33 Index) Energy Consumption Limit (kWh/year)	274.73
A++ Energy Level (33 Index) Energy Consumption Limit (kWh/day)	0.753

3.2.3 Refrigerator Energy Measurement Test and Standard

Refrigerators and freezers (and their combinations) are regulated for energy labeling all over the world based on different standards. For the present study, the European standard has been followed. The refrigerator energy consumption levels and volume measurements have been calculated with the help of ISO 15502 standards [13].

According to the standards, the refrigerating appliance is placed on a wooden platform painted black and open for free air circulation under the platform. The ambient temperature is measured at two points, T_{a1} and T_{a2}, located at the vertical and horizontal centerline of the sides of the refrigerating appliance and at a distance of 350 mm from the refrigerating appliance. The air temperature is measured using copper or brass cylinders placed 30 mm below the bottom of the platform. The

temperature value indicates the ambient temperature ± 1.0°C. The measurement point must be on the vertical axis through the geometrical center of the refrigerating appliance. The structure and the dimensions are shown in Figure 3.7. Ambient temperatures are kept constant within ± 0.5 K both during the periods required for obtaining stable operating conditions and during the tests. Unless otherwise is specified, the relative humidity should not exceed 75%.

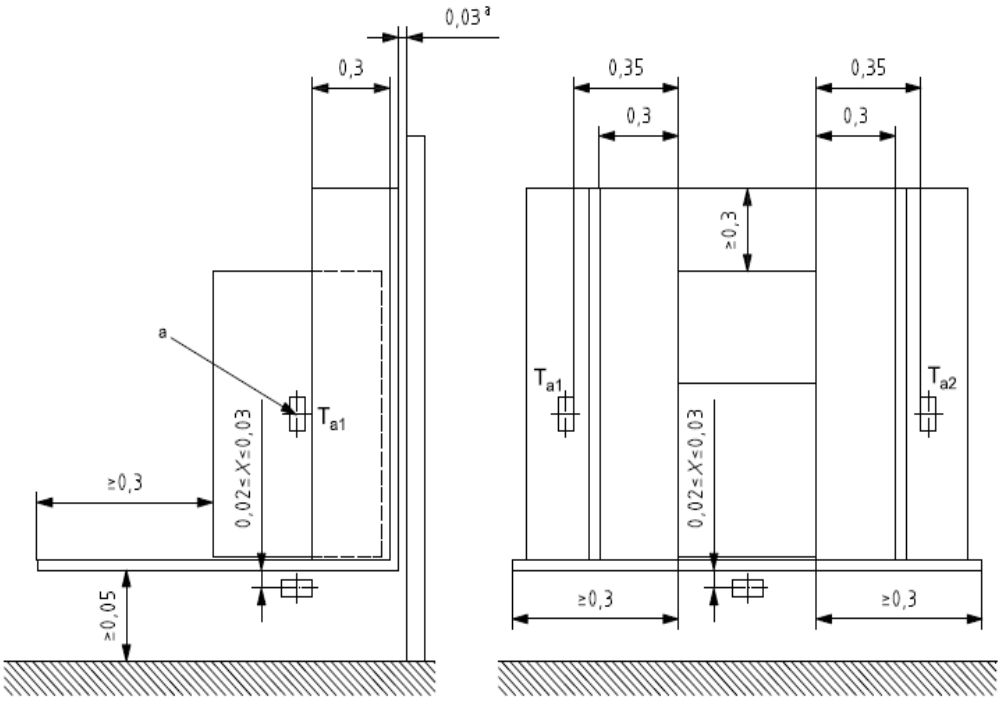

Figure 3.7 Prevention of air circulation and temperature measurement points [13, 14].

The refrigeration process needs to be capable of maintaining, simultaneously, the required storage temperatures in different compartments as given in Table 3.8 for different types of refrigerating appliances and for appropriate climate classes.

Table 3.8 Energy measurement tests: minimum required storage temperatures in different compartments [13, 14]

°C						
Fresh-food storage compartment		**Food freezer and three-star compartment/ cabinet**	**Two-star compartment/ section**	**One-star compartment**	**Cellar compartment**	**Chill compartment**
t_{1m}, t_{2m}, t_{3m}	t_{ma}	t^{***}	t^{**}	t^{*}	t_{cm}	t_{cc}
$0 \leqslant t_{1m}, t_{2m}, t_{3m} \leqslant 8$	$\leqslant +4$	$\leqslant -18$ [a]	$\leqslant -12$ [a]	$\leqslant -6$	$+8 \leqslant t_{cm} \leqslant +14$	$-2 \leqslant t_{cc} \leqslant +3$

The selected refrigerator for the experimental study has fresh food, chiller and freezer compartments. For the fresh food compartment the thermocouples are located at points labeled as T_1, T_2, T_3 as shown in Figure 3.8, halfway between the rear internal wall of the appliance and the internal wall of the closed door. For determining the temperatures in the chiller compartment, a storage plan is organized according to the standards. The temperature t_{cc} (cooling compartment) is always measured in M-packages (measurement packages) positioned or suspended with their largest surface horizontal at least 25 mm away from all walls and ceilings and from the other packages of the test load. For the freezer compartment, the temperatures are measured in M-packages, which are distributed throughout the load of test packages created for the refrigerator (Figure 3.9). The exact load of the test packages is given in Figure 3.10. The above measurements made during an operating cycle are recorded at intervals not greater than 60 s.

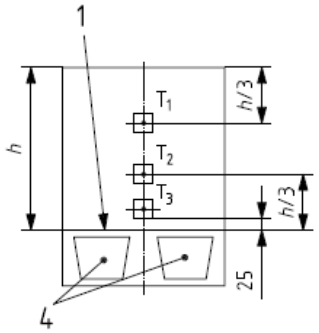

Figure 3.8 Temperature measurement points in fresh-food storage compartments [13, 14].

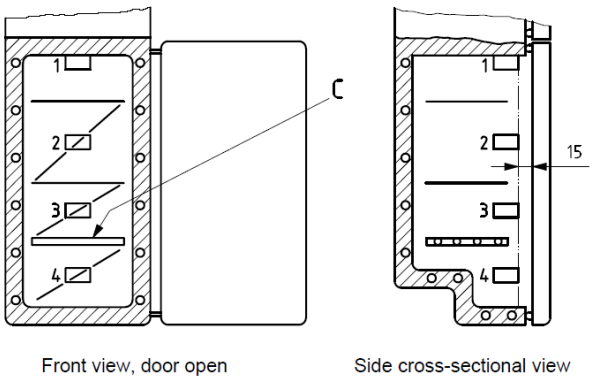

Figure 3.9 Sample loading plan for frozen storage compartment without unventilated, refrigerated walls and door shelves [13, 14]

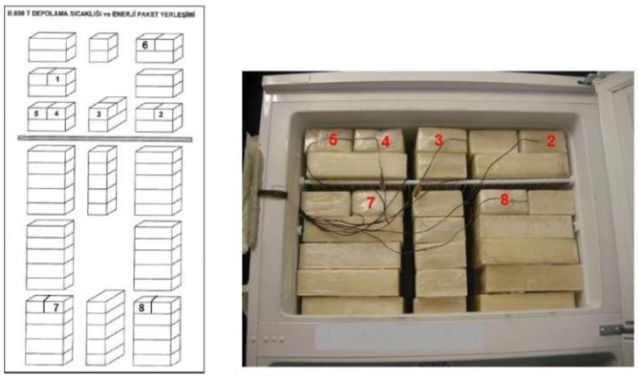

Figure 3.10 Experimentally investigated refrigerator loading plan for the frozen storage compartment.

3.3 Experimental Setup for the Solo Condenser Tests

After finishing the first part of the study, in order to perform a deeper analysis, condensers with horizontal tubes are considered. In the second part of the study solo condensers with different tube outer diameters and inclination have been prepared for experiments and placed in the test room provided by Arçelik A.Ş. Central Research and Development Center Fluid Mechanics Laboratories in Istanbul. In this exchanger test room, the heat capacity of solo heat exchangers can be measured with the usage of R600a. Thermocouples, air velocity transducers, pressure transducers and relative humidity sensors are located at locations imposed by the standards. Figure 3.11 shows a schematic of the experimental setup.

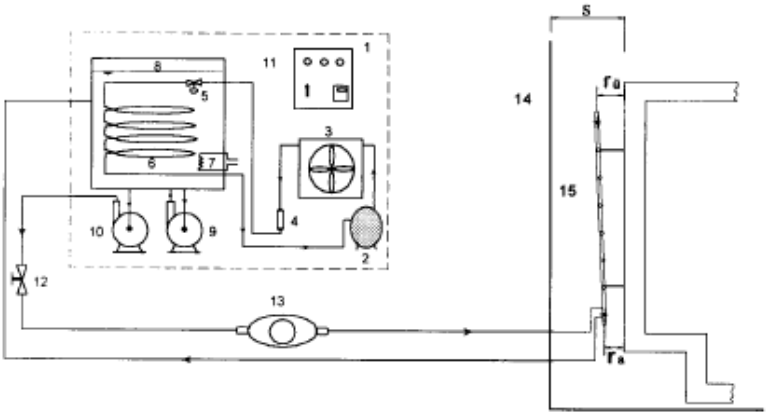

Figure 3.11 Schematic representation of the experimental setup for solo heat exchangers.

The experimental setup includes

1. Water Bath
2. Pump
3. Condenser
4. Dryer
5. Expansion Valve
6. Evaporator
7. Heater
8. Water Tank
9. Circulation Pump
10. Pump
11. Electrical Pane
12. Vane
13. Flow meter
14. Back wall
15. Test Exchanger
16. Refrigerator
17. Test Room
18. Data Logger
19. PC

3.4 Experimental Procedure for the Solo Condenser Tests

In the solo condenser tests, measurements are made during stable condition periods. When the stable conditions are reached, an experimental run takes about 80-90 minutes. During this period, the refrigerant flow rate is measured by a flow meter (Krohne Brand MFS 3000-1.5E) and is kept constant. The experiments are repeated for different tube outer diameters and for different inclinations. During the performance experiments, a total of twenty seven thermocouples have been used to record the temperature data at the following locations:

TC1- Expansion Valve Inlet
TC2- Evaporator Inlet
TC3- Eva Mid Pass
TC4- Eva Last 3 Pass
TC5- Eva Exit
TC6- Compressor Return
TC7- Compressor Exit
TC15- The Ambient Temp Right Side
TC16- Condenser Inlet Air1
TC17- Condenser Inlet Air2
TC18- Condenser Inlet Air3
TC19- Condenser Inlet Air4
TC20- Condenser Inlet Air5
TC21- Condenser Inlet Air6

TC8- Condenser Inlet

TC9- Condenser First Pass

TC10- Condenser Last 3 Pass

TC11- Condenser Last 2 Pass

TC12- Condenser Last Pass

TC13- Condenser Exit

TC14- The Ambient Temp Left Side

TC22- Condenser Exit Air1

TC23- Condenser Exit Air2

TC24- Condenser Exit Air3

TC25- Condenser Exit Air4

TC26- Condenser Exit Air5

TC27- Condenser Exit Air6

In order to determine the phase of the refrigerant, at the inlet and exit of the condenser pressure measurements are performed. The pressure measurement points are

DC1- Condenser Inlet

DC2- Expansion Valve Inlet (Condenser Exit)

In Figure 3.12, schematical representations of thermocouple and pressure transducer locations are given.

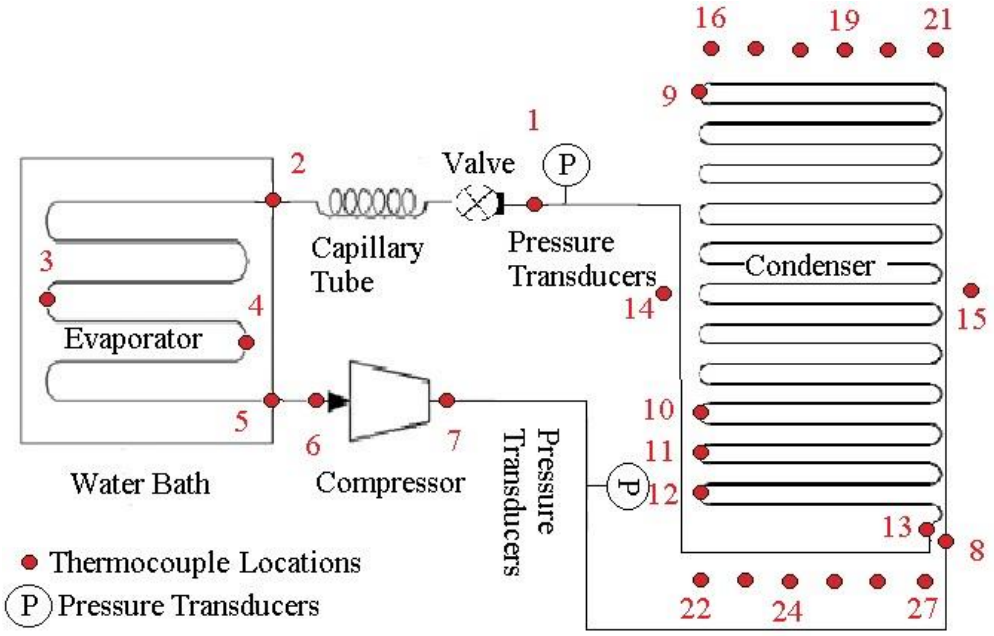

Figure 3.12 Schematic representation of thermocouples and pressure transducers locations in the experimental setup

CHAPTER 4

ANALYSIS OF TEST DATA

4.1 Refrigerator Experiments

4.1.1 Design of Experimental Matrix and Effective Parameter Analysis

As mentioned in Section 3.2, the effects of the following parameters have been investigated:

- Condenser tube outer diameter,
- Condenser inclination,
- Orientation of the tubes (vertical or horizontal).
- Amount of refrigerant

A total of sixteen experiments have been completed during this part of the study. In order to analyze the individual and combinational effects of various parameters, six sigma tools and Minitab statistical software have been used. In general usage, design of experiments (DOE) or experimental design is the design of any information-gathering exercises where variation is present, whether under the full control of the experimenter or not. Design of experiments is thus a discipline that has very broad applications across all the natural and social sciences and engineering.

For every different parameter, the refrigerator energy consumption measurements have been taken for about 3-5 days. After testing and measuring sixteen different parameters, Table 4.1 has been generated. The bold EEI values are below the upper limit of 33 for the A++ energy level.

Table 4.1 DOE Matrix Results

Condenser Outer Diameter (mm)	Condenser Inclination (1.5°)	Tube Orientation	Amount of Refrigerant (gr)	Daily Energy Measurement Results (kWh)	EEI Results
4	Yes	Horizontal	56	0.758	33.22
4	Yes	Horizontal	48	0.785	34.40
4	No	Horizontal	56	0.788	34.53
4	No	Horizontal	48	0.770	33.75
4.76	Yes	Horizontal	50	0.762	33.39
4.76	Yes	Horizontal	57	0.75	**32.87**
4.76	No	Horizontal	57	0.776	34.01
4.76	No	Horizontal	50	0.800	35.06
4	Yes	Vertical	48	0.756	33.13
4	Yes	Vertical	56	0.752	**32.96**
4	No	Vertical	48	0.764	33.48
4	No	Vertical	56	0.797	34.93
4.76	Yes	Vertical	50	0.777	34.05
4.76	Yes	Vertical	57	0.738	**32.34**
4.76	No	Vertical	57	0.769	33.70
4.76	No	Vertical	50	0.791	34.67

The investigated parameters such as the condenser tube diameter, condenser inclination, tube orientation, and the gas charge are called predictors, and the energy measurement is called the response in the analyses. The effect of each predictor is weighted based on their *p*-values determined from DOE. The *p*-value for each term tests the null hypothesis that the coefficient is equal to zero (no effect). A low *p*-value (< 0.05) indicates that you can reject the null hypothesis. In other words, a predictor that has a low *p*-value is likely to be a meaningful addition to your model because changes in the predictor's value are related to changes in the response variable. Conversely, a larger (insignificant) *p*-value suggests that changes in the predictor are not associated with changes in the response. From the output shown in Figure 4.1 (the Pareto chart) it can be observed that all of the predictors have *p*-values greater than the limiting value of 0.05, which indicates a statistically

insignificant effect. Hence, starting from 4-way interactions, the not effective interactions are removed from the DOE.

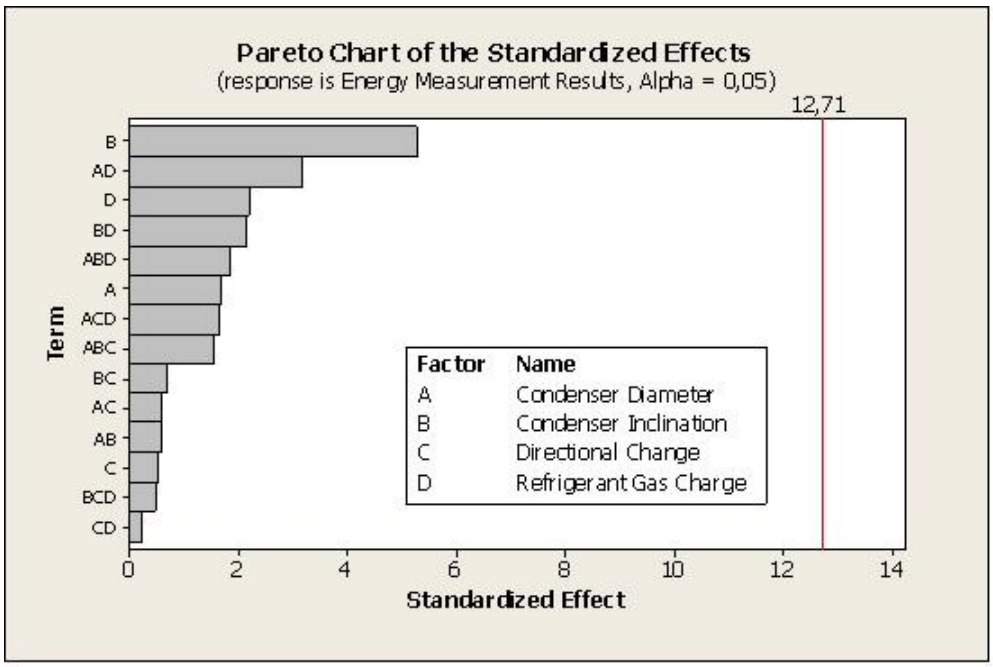

Source	F	P
Main Effects	9,14	0,243
Condenser Diameter	2,81	0,342
Condenser Inclination	27,89	0,119
Directional Change	0,30	0,682
Refrigerant Gas Charge	4,88	0,271
2-Way Interactions	2,61	0,441
Condenser Diameter*Condenser Inclination	0,34	0,663
Condenser Diameter*Directional Change	0,36	0,656
Condenser Diameter*Refrigerant Gas Charge	10,12	0,194
Condenser Inclination*Directional Change	0,47	0,618
Condenser Inclination*Refrigerant Gas Charge	4,55	0,279
Directional Change*Refrigerant Gas Charge	0,05	0,857
3-Way Interactions	2,13	0,470
Condenser Diameter*Condenser Inclination*Directional Change	2,41	0,364
Condenser Diameter*Condenser Inclination*Refrigerant Gas Charge	3,44	0,315
Condenser Diameter*Directional Change*Refrigerant Gas Charge	2,62	0,352
Condenser Inclination*Directional Change*Refrigerant Gas Charge	0,23	0,714
Residual Error		
Total		

Figure 4.1. Main effects plot and Pareto chart of DOE analysis.

After removing non-effective parameters one by one, the Pareto chart in Figure 4.2 is obtained. The chart covered 95.84% of the entire experimental variations.

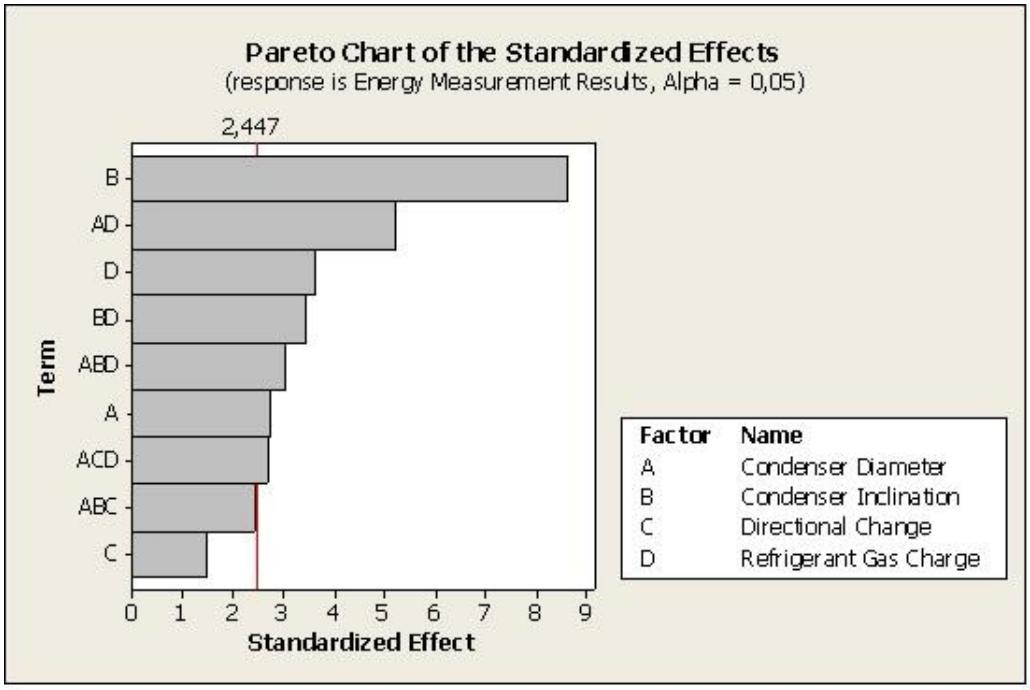

Source	F	P
Main Effects	24,91	0,001
Condenser Diameter	7,63	0,033
Condenser Inclination	74,77	0,000
Directional Change	2,19	0,189
Refrigerant Gas Charge	13,22	0,011
2-Way Interactions	19,64	0,002
Condenser Diameter*Refrigerant Gas Charge	27,43	0,002
Condenser Inclination*Refrigerant Gas Charge	11,85	0,014
3-Way Interactions	7,52	0,019
Condenser Diameter*Condenser Inclination*Directional Change	6,00	0,050
Condenser Diameter*Condenser Inclination*Refrigerant Gas Charge	9,30	0,023
Condenser Diameter*Directional Change*Refrigerant Gas Charge	7,25	0,036
Residual Error		
Total		

S = 0,00581706 PRESS = 0,00137945
R-Sq = 95,84% R-Sq(pred) = 71,75% R-Sq(adj) = 89,60%

Figure 4.2. Main effects plot and Pareto chart of DOE analysis after elimination of non-effective parameters

After the elimination of the non-effective parameters, DOE analysis yields the main effects, some of the two-way and three-way interactions. The related results are presented and discussed in Chapter 5

.

4.2 Solo Condenser Experiments

4.2.1 General

The data recorded during the experiments described in Chapter 3 have been used to calculate the total capacity, overall heat transfer coefficient, and equivalent outside heat transfer coefficient of the wire-and-tube type refrigerator condensers. The complex structure of the condenser does not allow analytical solutions. Hence, with varied tube outer diameters and condenser inclinations, in order to evaluate the heat transfer characteristics, empirical correlations are used. The fin efficiencies are taken from the literature [9].

4.2.2 Method of Calculation

The mass flow rate of the refrigerant was read from the flowmeter in the experimental setup. The total heat rejected from the condenser was determined by calculating the overall heat transfer coefficient.

The refrigerant inside the condenser can be in three different phases, namely, the superheated vapor (in the desuperheating section), saturated vapor, and subcooled liquid phases. In these regions, the condenser performance has to be assessed differently. In the end there would be three UA values to be obtained.

4.2.2.1 Calculation of Heat Transfer Rates

The total heat transfer rate from the condenser can be expressed as

$$\dot{Q} = \dot{Q}_{sup} + \dot{Q}_{two} + \dot{Q}_{sub} \tag{4.1}$$

where

$\dot{Q}_{\text{desup}}$: Desuperheating region heat transfer rate

$\dot{Q}_{\text{two}}$: Two phase (condensation) region heat transfer rate

$\dot{Q}_{\text{sub}}$: Subcooled region heat transfer rate

$$\dot{Q}_{sup} = \dot{m}_r\left(h_{in} - h_g\right) \quad (4.2)$$

$$\dot{Q}_{two} = \dot{m}_r h_{fg} \quad (4.3)$$

$$\dot{Q}_{sub} = \dot{m}_r(h_f - h_{out}) \quad (4.4)$$

where

$\dot{m}_r$: Refrigerant flow rate inside the condenser tube (kg/s)

h_{in}: Enthalpy of the refrigerant which enters the condenser (kJ/kg)

h_g: Enthalpy of saturated vapor refrigerant at condensation temperature (kJ/kg)

h_{fg}: Latent heat of phase change of refrigerant at condensation temperature (kJ/kg)

h_f: Enthalpy of saturated liquid refrigerant at condensation temperature (kJ/kg)

h_{out}: Enthalpy of the refrigerant which leaves the condenser (kJ/kg)

4.2.2.2 Calculation of Inside Convective Heat Transfer Coefficients

Several correlations have been reported in the literature for the inside convective heat transfer coefficient. The Reynolds number may be evaluated from the relation

$$Re_D = \frac{4\dot{m}_r}{\pi D_{t,in}\mu} \quad (4.5)$$

where μ is the dynamic viscosity of the refrigerant.

For the desuperheating region (turbulence flow *Re* > 2300) from Dittus-Boelter Equation

$$h_{\text{i, Db}} = \frac{k_v}{d_{t,in}} 0.023 \left(\frac{4\dot{m}_r}{\pi d_{t,in}\mu_v}\right)^{0.8} \left(\frac{\mu_v c_{pv}}{k_v}\right)^{0.3} \quad (4.6)$$

where,

k_v: Thermal conductivity of the refrigerant which enter the condenser (W/mK),

C_{pv}: Specific heat of the refrigerant (kJ/kgK).

Also for the Gnielinski correlation,

$$f = (0.79 \ln Re - 1.64)^{-2} \tag{4.7}$$

$$h_{i,G} = \frac{k}{d_{t,in}} \frac{\frac{f}{8}(Re-1000)Pr}{1+12.7\left(\frac{f}{8}\right)^{0.5}\left(Pr^{2/3}-1\right)} \tag{4.8}$$

For two phase region from Cavallini and Zecchin,

$$h_{i,Cz} = \frac{k_l}{d_{t,in}} 0.05 Re_{eq}^{0.8} \left(\frac{\mu_l c_{pl}}{k_l}\right)^{0.33} \tag{4.9}$$

where, l represents liquid phase of the refrigerant.

$$Re_{eq} = Re_l + Re_v \frac{\mu_v}{\mu_l}\left(\frac{\rho_l}{\rho_v}\right)^{0.5} \tag{4.10}$$

$$Re_l = \frac{4\dot{m}(1-x)}{\pi d_{t,in}\mu_l} \qquad Re_v = \frac{4\dot{m}x}{\pi d_{t,in}\mu_v} \tag{4.11}$$

For every different x values $0 \leq x \leq 1$, $h_{i,Cz}$ can be calculated and an average heat transfer coefficient can be obtained from the equation

$$\overline{h_{l,Cz}} = \frac{1}{L}\int_0^L h_{i,Cz} dL \tag{4.12}$$

For the subcooled region, laminar flow assumption has been made. The length of the subcooled region has been determined for the condensers wıth tubes of the original length and the shortened length. Then, the thermal entry length has been calculated. The fully developed conditions are valid for $[(x/D_t)/Re_D Pr] \approx 0.05$ [15]. For constant temperature conditions, Sieder and Tate [16] suggested Equation 4.14 for the calculation of $\overline{Nu_D}$. All properties, except μ_s, should be evaluated at the mean temperature $((T_{satout}+T_{out})/2)$.

$$Pr = {C_p \mu}/{k} \tag{4.13}$$

$$\overline{Nu_D} = 1.86 \left(\frac{Re_D Pr}{L/d_{t,in}}\right)^{1/3} \left(\frac{\mu}{\mu_s}\right)^{0.14} \tag{4.14}$$

$$h_{i,sub} = \frac{k_l}{d_{t,in}} \overline{Nu_D} \tag{4.15}$$

(4.14) is recommended for use when $0.60 \leq Pr \leq 5$ and $0.0044 \leq (\mu/\mu_s) \leq 9.75$ provided. If $\overline{Nu_D}$ falls below 3.66, it is reasonable to use $\overline{Nu_D}$=3.66 since fully developed conditions are valid.

4.2.2.3 Calculation of Outside Convective Heat Transfer Coefficients

The condenser which was experimentally investigated can be divided into two sections, the first part includes the vertical flow without interference with fins and the second part includes the horizontal flow interference with fins. The tube lengths corresponding to the desuperheating, condensation, and subcooled regions have been calculated using thermocouples at the inlet and outlet sections of the condensers. For every twenty centimeters of the condenser tube, one thermocouple has been mounted. The experimentally investigated condenser and the assembled thermocouples are given in Figure 4.3. By measuring the difference between each thermocouple reading, the tube lengths for each regime have been calculated. Based on the temperature readings, the regions of phase transition are determined and the thermocouple locations have been modified to take more frequent measurements in this regions. This enables the precise determination of the length of each regime.

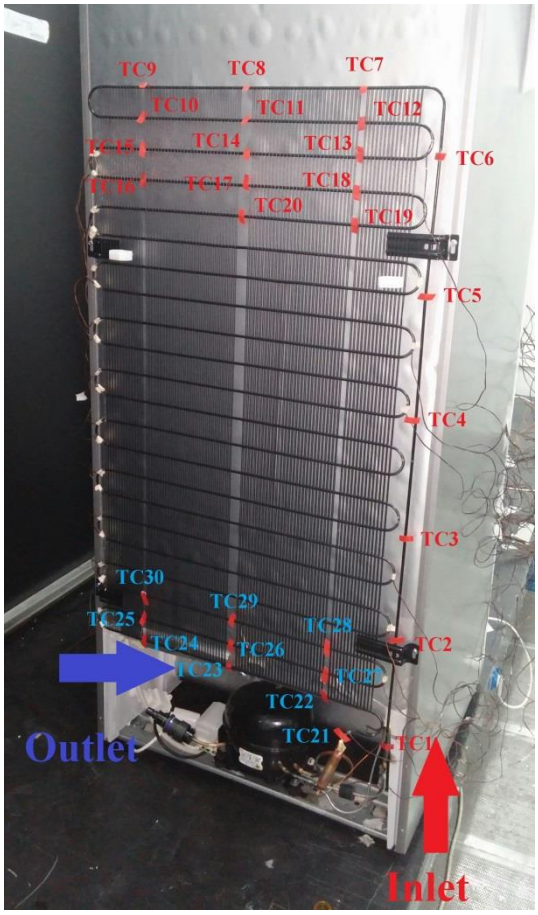

Figure 4.3 Determination of the tube lengths corresponding to the desuperheating, condensation, and subcooled regions.

The tube lengths corresponding to the desuperheating, condensation, and subcooled regions for every tested condenser are given in Table 4.2. and are schematically shown in Figure 4.4.

Table 4.2 Determined Tube Lengths of Each Region

	Original Length (*L*=15.85m)	**Original Length (*L*=15.85m)**	**Shortened Length (*L*=13.36m)**
Desuperheating Region Length L_{desup} (m)	1.40	1.40	1.30
Phase Change Region Length L_{two} (m)	12.40	11.70	11.60
Subcooled Region Length L_{sub} (m)	2.05	2.75	0.46

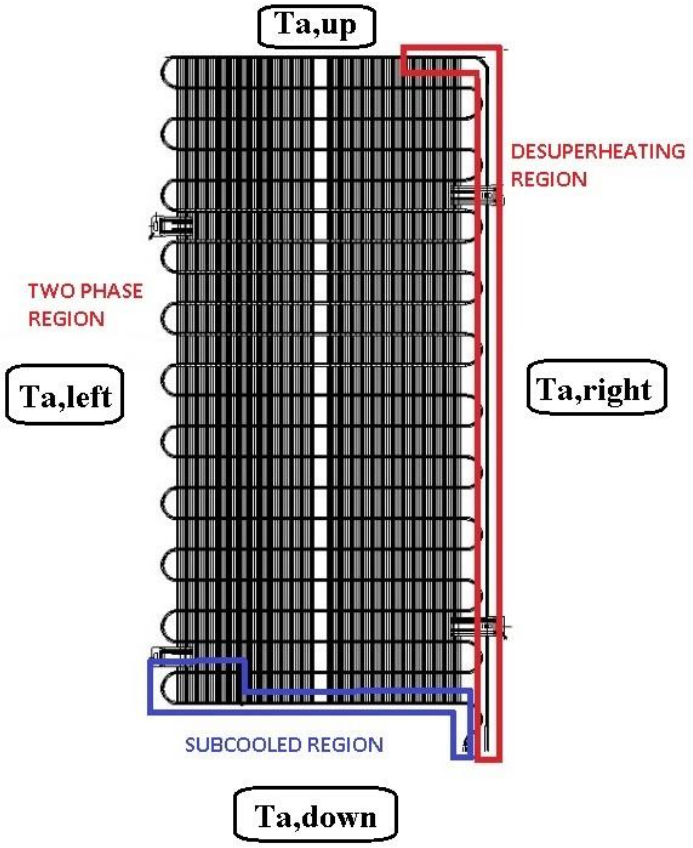

Figure 4.4 Experimentally determined flow characteristics inside the condenser and surrounding air temperature measurement locations.

The experimental measurements indicated that the desuperheating region approximately occupied the whole vertical part of the condenser tube. For a vertical tube, the air side convective heat transfer coefficient can be calculated using

$$h_o = \frac{\dot{Q}_{sup}}{A_t \frac{T_{in}-T_{sat}}{\ln \frac{T_{in}-T_{a,right}}{T_{sat}-T_{a,right}}}} \tag{4.16}$$

For the two phase and subcooled regions the following correlations from the literature [4, 5] have been employed.

$$Nu = 0.4724 Gr^{0.2215} \tag{4.17}$$

$$Gr = \frac{{D_c}^3 \rho_a^2 g \beta (T_{sat}-T_{amb})}{\mu_a^2} \tag{4.18}$$

where;

ρ_a: Density of air $(\mathrm{kg/m^3})$

g: Gravitational acceleration $(\mathrm{m/s^2})$

μ_a: Dynamic viscosity of air (Pa.s)

β: Coefficient of thermal expansion given for and ideal gas (air)

$$\beta = \frac{1}{\left(\frac{(T_{sat}+T_{amb})}{2}+273.15\right)} \tag{4.19}$$

D_c:Characteristic Length

$$D_c = \frac{\frac{S_w}{S_t}D_0^2+D_w^2}{\frac{S_w}{S_t}D_0+D_w} \tag{4.20}$$

$$h_o = \frac{Nuk_a}{D_c} \tag{4.21}$$

k_a: Air thermal conductivity

Defining appropriate mean temperature differences for the three different regions is important. The logarithmic mean temperature has been used to calculate the overall heat transfer coefficient in the desuperheating and subcooled regions. For the two phase region, the temperature difference has been employed.

$$\Delta T_{\mathrm{lm,desup}} = \frac{T_{T,in}-T_{T,sat}}{\ln\left(\frac{T_{T,in}-T_{a,right}}{T_{T,sat}-T_{a,right}}\right)} \tag{4.22}$$

$$\Delta T_{\mathrm{lm,sub}} = \frac{T_{T,sat}-T_{T,out}}{\ln\left(\frac{T_{T,sat}-T_{amb}}{T_{T,out}-T_{amb}}\right)} \tag{4.23}$$

where

T_{amb}: Temperature of the air surrounding test setup (°C) which is calculated from the experimental data as

$$T_{amb} = \frac{T_{a,down}+T_{a,up}+T_{a,left}+T_{a,right}}{4} \quad (4.24)$$

4.2.2.4 Calculation of *UA* Values and Overall Heat Transfer Coefficients

Overall heat transfer coefficients for every different section have been calculated as follows.

$$\frac{1}{(UA)_{o,sect}} = \frac{1}{h_{i,sect}A_{t,insect}} + \frac{\ln(D_{t,out}/D_{t,in})}{2\pi k_t L_{t,sect}} + \frac{1}{h_{o,sect}(A_{t,outsect}+\eta_f A_{w,sect})} \quad (4.25)$$

where;

$A_{o,sect}$ is the total outer area of the test condenser section in m^2 as previously given in Table 3.1.

$A_{t,insect}$: Tube inner surface area of the section (m^2)

$h_{i,sect}$: Refrigerant side convective heat transfer coefficient of the section ($W/m^2.K$)

$A_{t,outsect}$: Tube outer surface area of the section (m^2)

$h_{o,sect}$: Air side convective heat transfer coefficient of the section ($W/m^2.K$)

$A_{w,sect}$: Wire area of the section (m^2)

The fin efficiency can be expressed as

$$\eta_f = \frac{\tanh\left(mS_t/2\right)}{m\frac{S_t}{2}} \quad (4.26)$$

where

$$m = \sqrt{\frac{4h_o}{k_w d_w}} \quad (4.27)$$

There are two approaches to calculate the total overall heat transfer of experimentally investigated condensers. These two approaches are shared in Chapter 5.

4.3 Second Stage Refrigerator Experiments

4.3.1 Systematic of the Experiments

In the first part of the study DOE analyses have been completed and experimental results have been analyzed. In the last part of the study, in order to further investigate about the effect of tube diameter, additional four experiments have been planned. In these experiments, by keeping the total covered area of the condenser the same, and having the same total outer surface area of the condenser (shaded in Table 4.3), the length of 4.76 mm tube has been shortened and the tube spacing has been increased. The shortened version of the condenser has 2.5 meters less tube length. In this configuration, the tubes have been bended and welded manually. The tube diameters, lengths, spacing details and areas are given in Table 4.3.

Table 4.3 Dimensions and Area Details of the Original and Shortened Tube Condensers

	Original Length (*L*=15.85m)	**Original Length (*L*=15.85m)**	**Shortened Length (*L*=13.36m)**
Tube Outer Diameter D_{to} (mm)	**4.76**	**4**	**4.76**
Tube Inner Diameter D_{ti} (mm)	3.36	3	3.36
Tube Spacing S_t (mm)	60	60	74
Number of Passes, n_t	22	22	18
Total Tube Length L_t (mm)	15850	15850	13363
Wire Diameter D_w (mm)	1.3	1.3	1.3
Wire Length L_w (mm)	1260	1260	1260
Number of Wires n_w	108	108	108
Wire Spacing S_w (mm)	10	10	10
Wire Perimeter P_w (mm)	4.084	4.084	4.084
Width of Condenser W (mm)	630	630	622
Height of Condenser H (mm)	1260	1260	1280
Total Tube Inner Area A_{ti} (m^2)	0.167	0.149	0.141
Total Tube Outer Area A_{to} (m^2)	0.191	**0.160**	**0.162**
Total Wire Area A_w (m^2)	0.556	0.556	0.556
Total Outer Area A_o (m^2)	0.747	0.716	0.718

CHAPTER 5

RESULTS AND DISCUSSION

5.1 Results

In this chapter the results of the experiments are presented and discussed. Sample experimental results of one of the refrigerator test (4mm outer tube diameter, horizontal tube orientation, 1.5° inclination, and 56 gr refrigerant) are given in Figures 5.1-7.

Figure 5.1 gives the change in temperature with time inside the fresh food compartment measured by four thermocouples in top, bottom, cover, vegetable sections. In the energy consumption tests, the average of the bottom, top and cover thermocouple readings must be less than or equal to 5°C [13, 14]. An average reading of about 4.5°C has been realized during the tests as indicated in Figure 5.2. In Figure 5.3 the thermocouple measurements for the five M-packages are illustrated, they are all below -18°C as required by the standard [13, 14].

The temperature measurements in the last three passes of the condenser are shown in Figure 5.4. The stability of the temperatures in this figure ensures that all components in the refrigeration system function properly. Figure 5.5 is a detailed view of Figure 5.4 for clarity.

Figure 5.6 indicates the power consumption of the refrigerator during the on and off times of the compressor. The stable operation of the cycle is also evident in Figure 5.6.

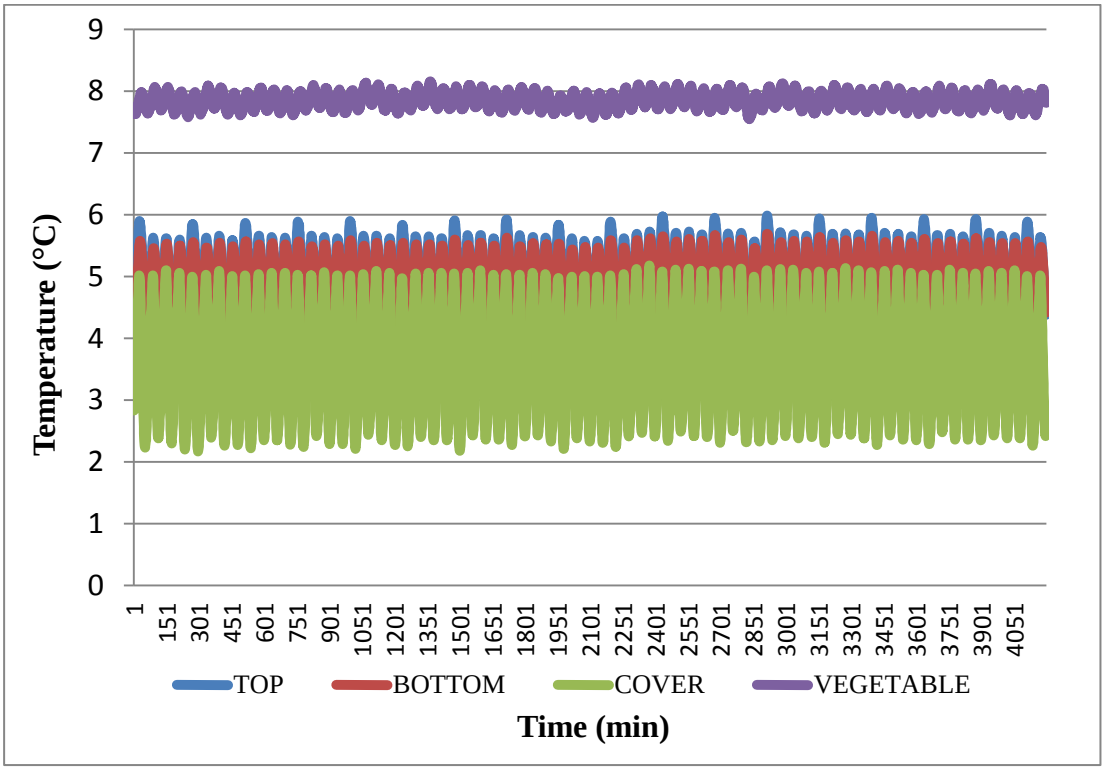

Figure 5.1 Freshfood compartment temperature variation with time

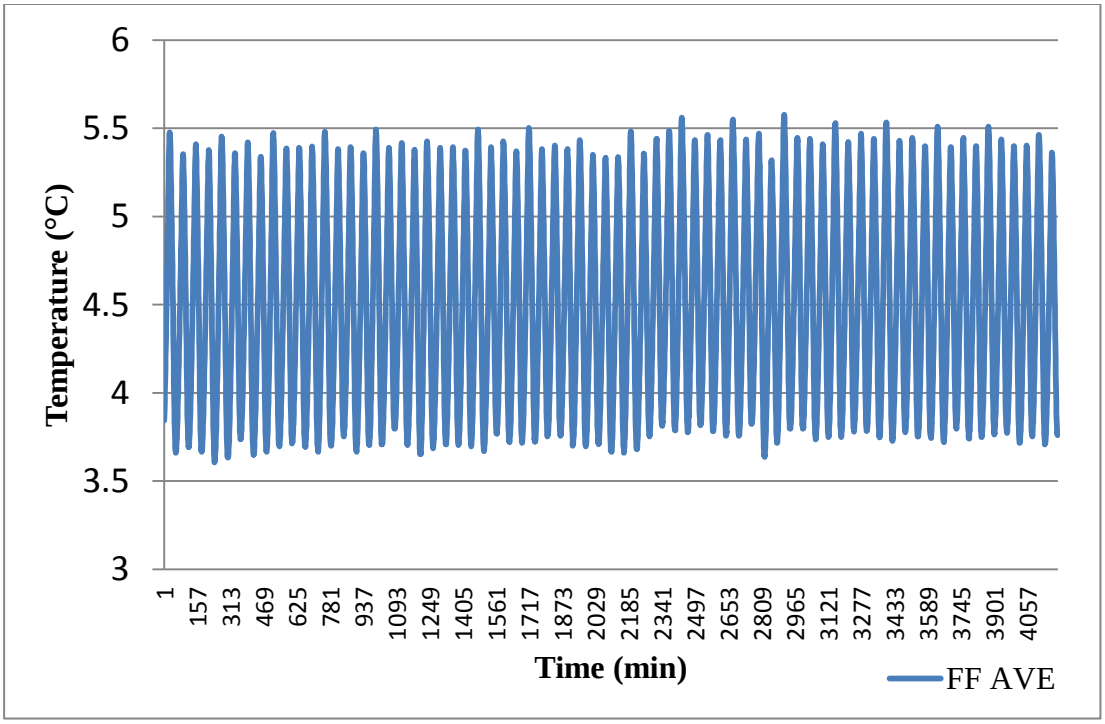

Figure 5.2 Freshfood average temperature variation with time

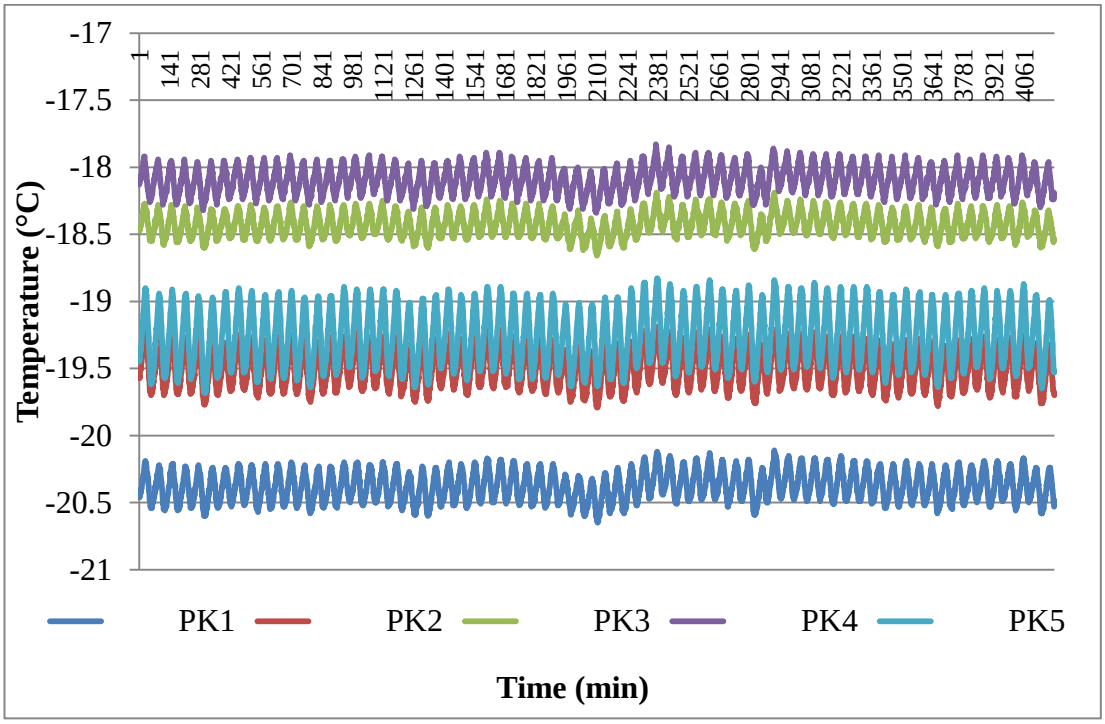

Figure 5.3 Freezer compartment temperature variation with time

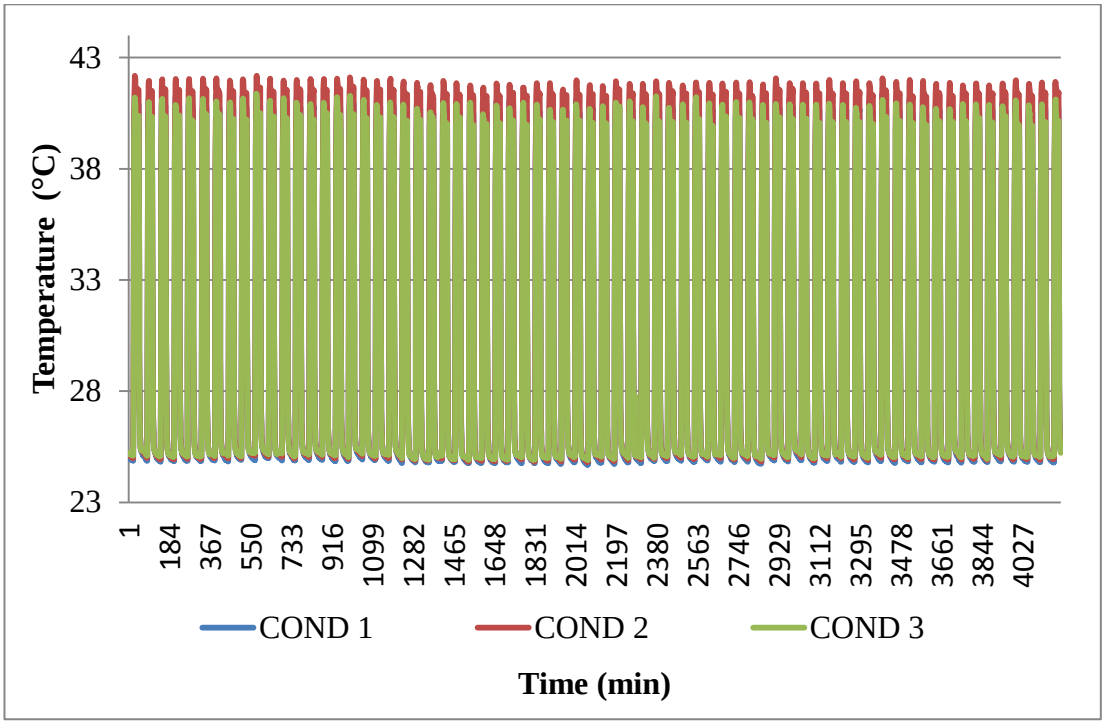

Figure 5.4 Condenser temperature variation with time

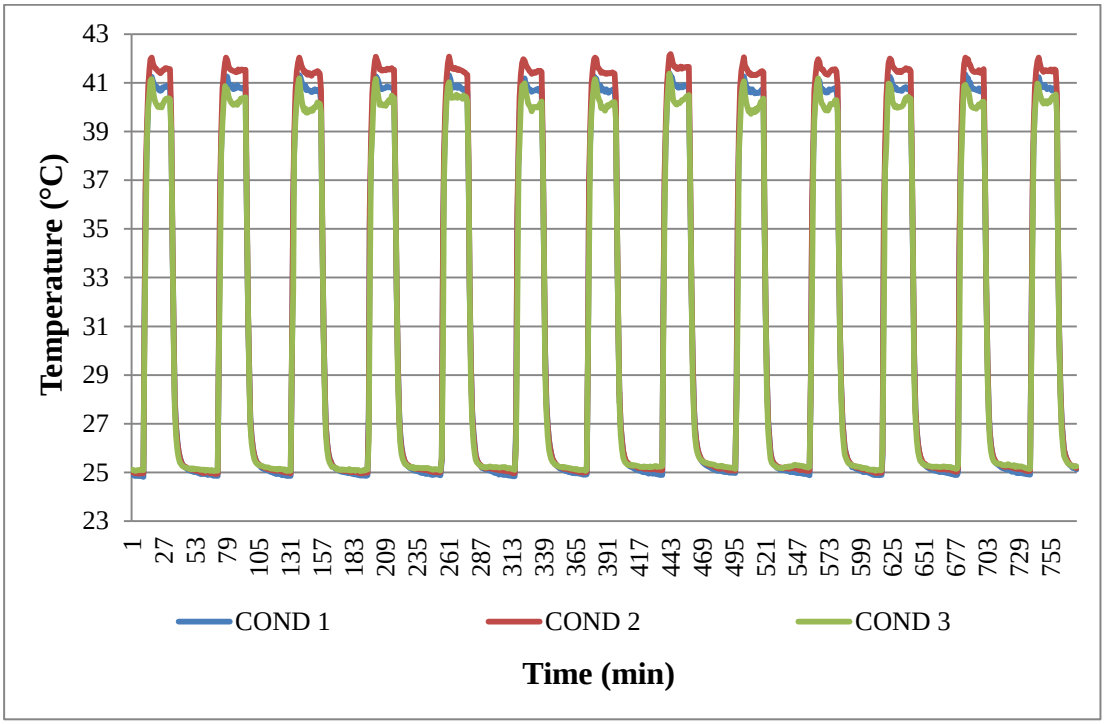

Figure 5.5 Detailed condenser temperature variation with time

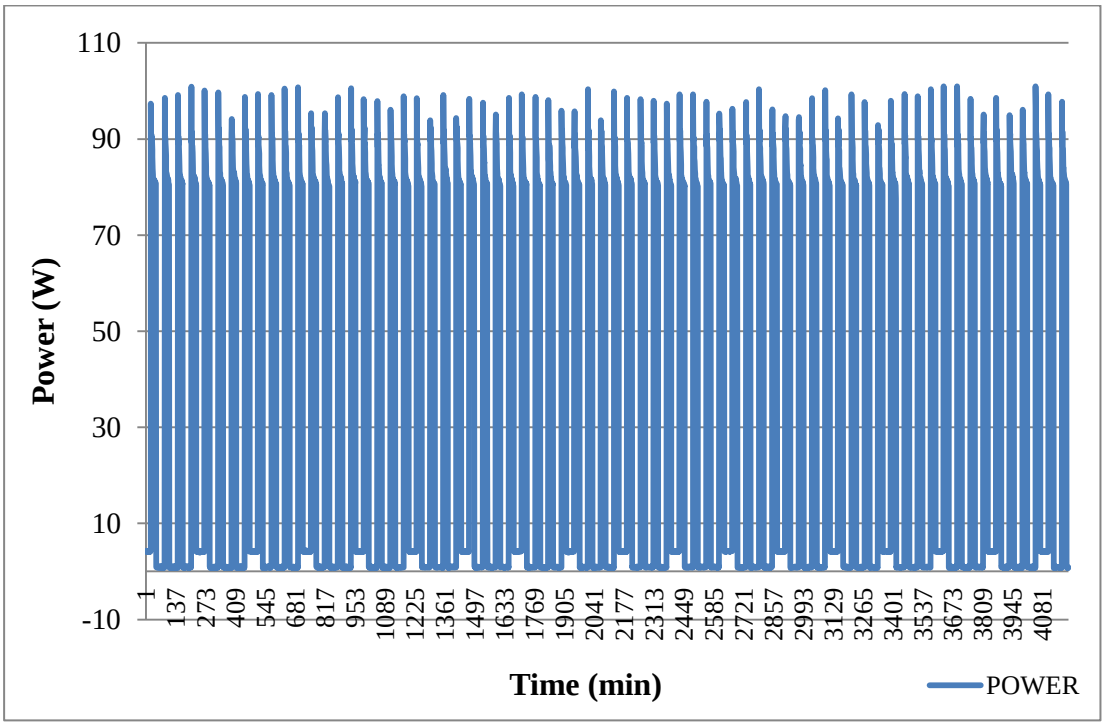

Figure 5.6 Power consumption variation with time

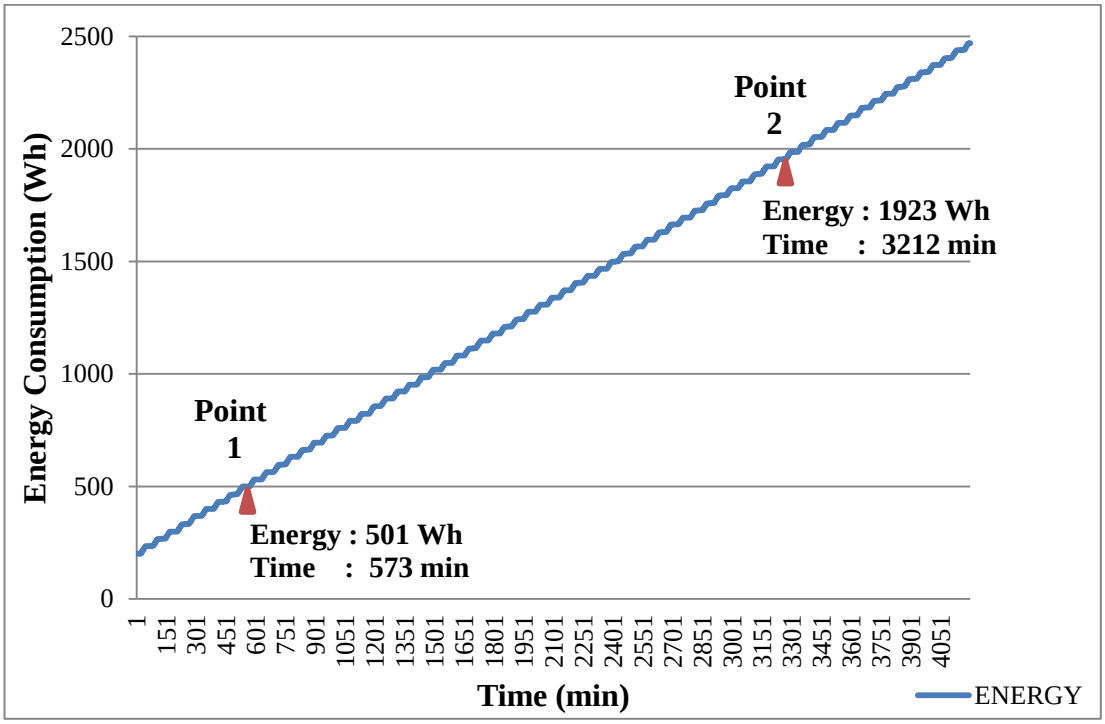

Figure 5.7 Energy consumption in time

Energy consumed by a refrigerating appliance is calculated over a period of 24 hours using the following formula.

$$E_{24h} = \frac{(E_{point2} - E_{point1})}{(t_{point2} - t_{point1})} 1440 \text{ min/24h} \quad (5.1)$$

where

E_{24h}: Energy consumption of household refrigerating appliance in kWh/24 h

The results of all sixteen refrigerator energy consumption tests are analyzed and discussed next.

5.1.1 Refrigerator Tests Statistic Minitab Software Results

Since the effects of four different parameters have been investigated in the present study, after the elimination of non-effective parameters, the DOE analyses have shown the main effects, some of the 2-way interactions and some of the 3-way interactions. The results are presented Figures 5.8 and 5.9.

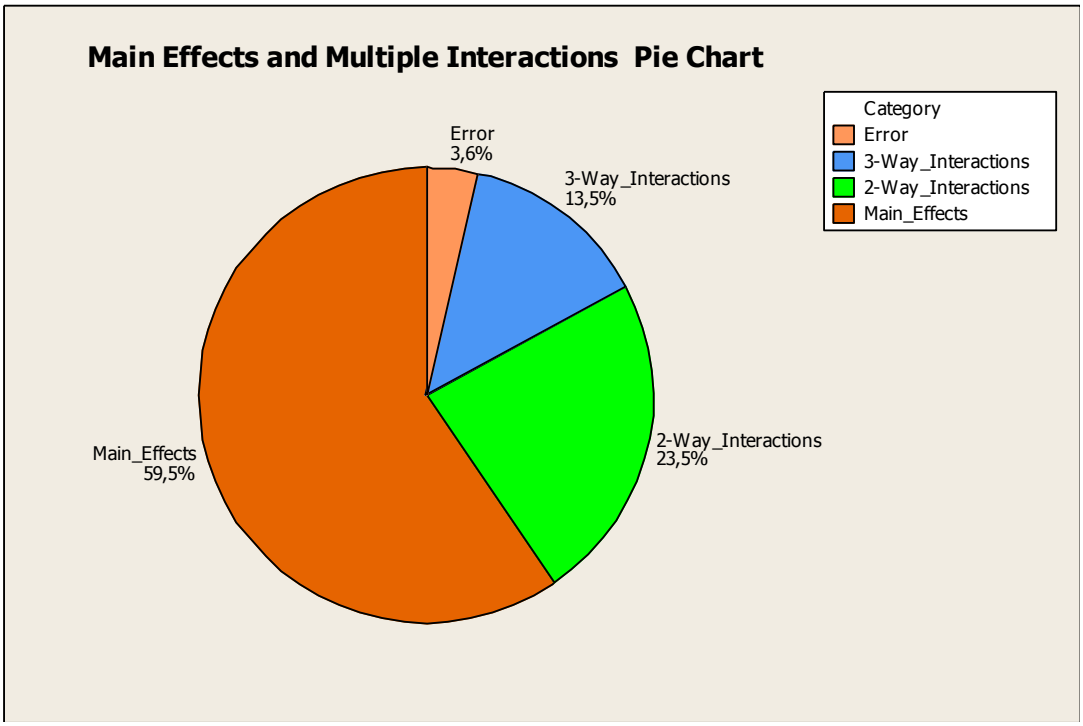

Figure 5.8 Design of experiment results: the main effects and multiple interactions pie chart

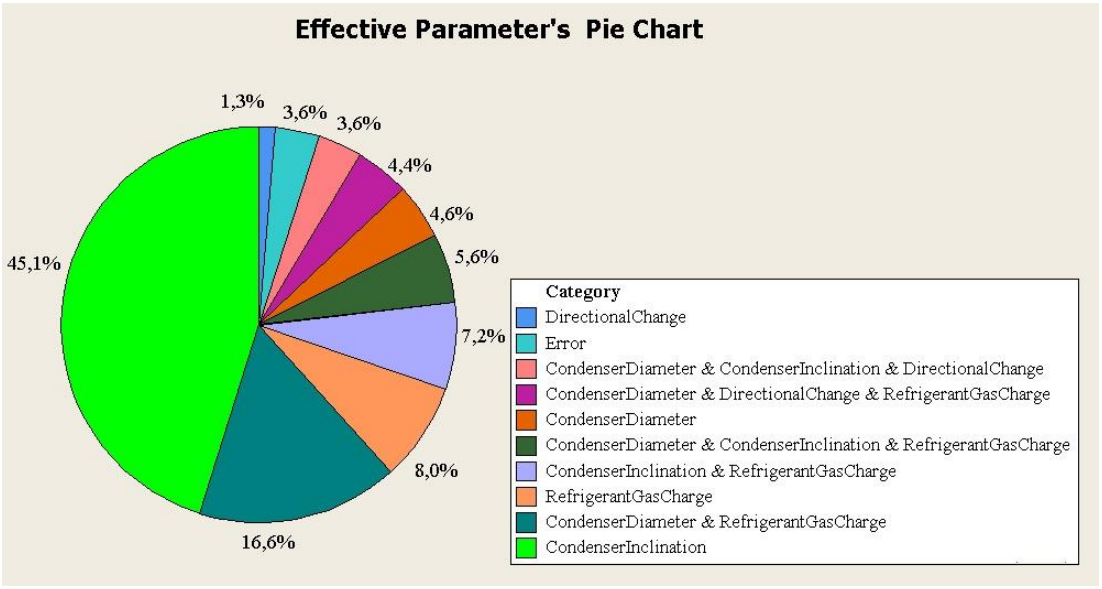

Figure 5.9 Design of experiment results: effective parameters pie chart

According to DOE results shown in Figure 5.8, 59.5% of the improvement on the refrigerator energy consumption comes from the variation of the main effects. 2-way effects have also 23.5% influences on the experiments. When the results are carefully analyzed, it can be seen that the condenser inclination has 45.1% effect on

the defined experimental parameters to reduce the energy consumption of the refrigerators. The tube diameter and the refrigerant gas charge 2-way effect also has 16.6% influences on the energy consumption.

In order to analyze the effects of the parameters comparatively, Figure 5.10 has been plotted. It is observed from Figure 5.10 that the condenser inclination is the most effective parameter that reduces the energy consumption. Also the orientation of the tubes has a slight effect on the energy measurement results.

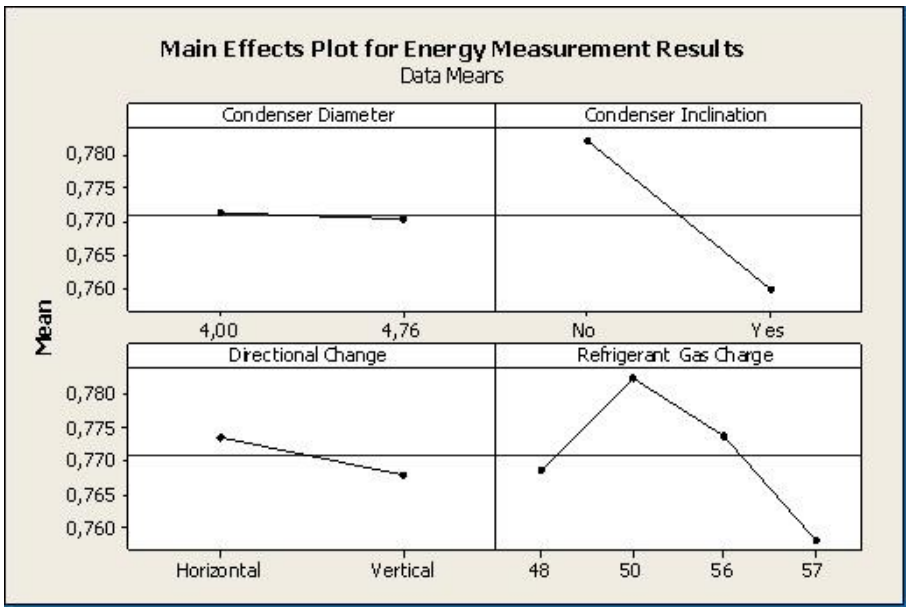

Figure 5.10 Main effects plot for energy measurement results

Based on DOE analysis, as the inclined condensers always performed better in terms of energy consumption, the DOE matrix has been divided into two sets: with and without inclination. A statistical analysis has been performed for the data including the condenser inclination. The new matrix is shown in Table 5.1.

Table 5.1 Subset of the Experimental Matrix for the Effects of Condenser Inclination

Condenser Outer Diameter (mm)	Condenser Inclination (1.5°)	Tube Orientation	Amount of Refrigerant (gr)	Daily Energy Measurement Results (kWh)	EEI Results
4	Yes	Horizontal	56	0.758	33.23
4	Yes	Horizontal	48	0.785	34.42
4.76	Yes	Horizontal	50	0.762	33.41
4.76	Yes	Horizontal	57	0.75	**32.88**
4	Yes	Vertical	48	0.756	33.15
4	Yes	Vertical	56	0.752	**32.97**
4.76	Yes	Vertical	50	0.777	34.07
4.76	Yes	Vertical	57	0.738	**32.36**

The uncertainty analysis of climatic room is shared in Appendix A. According to the power consumption measurements, climatic room data acquisition system is capable to measure results in the range of $\pm$ 0.001 kWh. Hence, energy consumption and their differences on the DOE setup are significant. The results of this analysis are shown in Figure 5.11 Condensers of vertical tubes with inclination clearly reduce the energy consumption. Condensers with 4 millimeter tube outer diameters show different performances for the horizontal and vertical orientation of the tubes. However, for the 4.76 millimeter tube outer diameter, it is difficult to observe a trend in the variation of energy consumption with the tube orientation at different charge values. A higher gas charge with condenser inclination has a positive effect on reducing the energy consumption. In Figure 5.11 the plot showing the two way interactions of the tube orientation (indicated as directional change on the figure), and the refrigerant gas charge might include an experimental error. The data for 48 g charge with vertical tubes is believed to be an erroneous data. For the future verification this experiment is to be performed again. It is clearly seen that the diameter change on the horizontal type of condenser changes the energy consumption. Therefore, in the second part of the study, solo condensers of horizontal tubes of different diameters and lengths have been investigated.

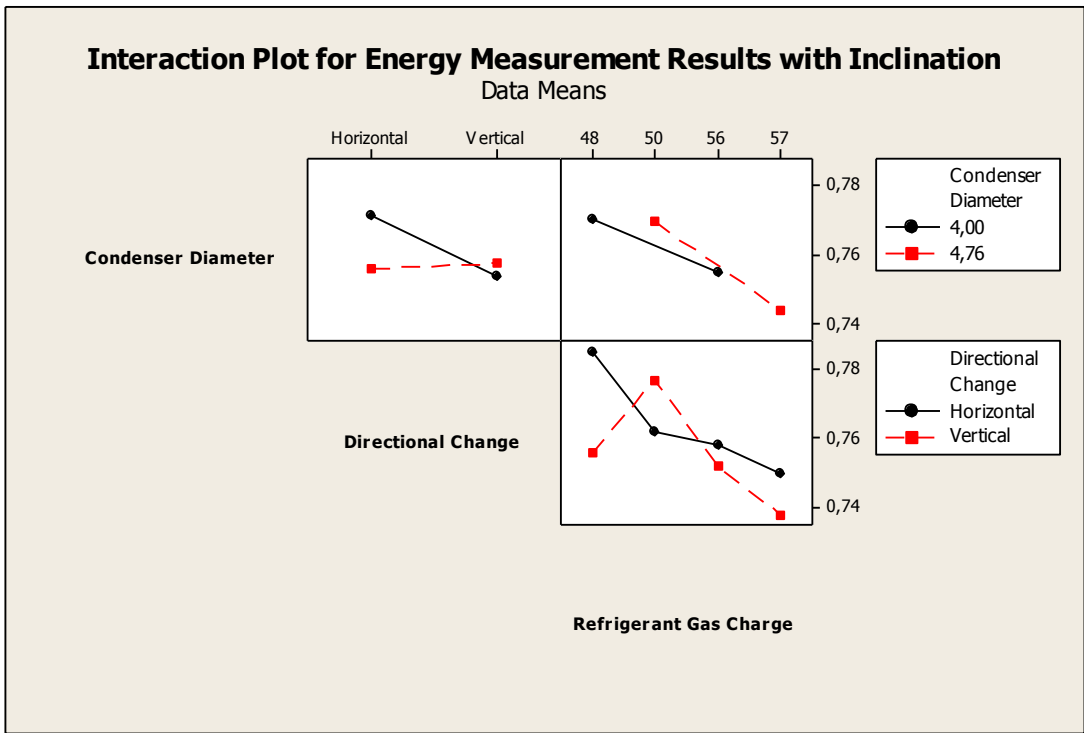

Figure 5.11 Interaction plot for energy measurement results with condenser inclination.

5.1.2 Solo Condenser Results

The first part of the refrigerator experiments indicated that the performance of the condensers with horizontal tubes is affected by tube outer diameter. In the solo condenser tests, three different types of condensers have been tested: one with a tube outer diameter of 4.76 mm of the original length; one with 4.76 mm diameter tubes of shortened length; and one 4 mm diameter tubes of the original length. The measured mass flow rate, condenser inlet, outlet temperatures and ambient temperatures are shared in Table 5.2. In this section, the heat transfer rate, the inside and airside convective heat transfer coefficients, and the overall heat transfer coefficient have been calculated for each different phase. Sample calculations for this section can be found in Appendix B.

Table 5.2 Experimentally Measured Mass Flow Rate and Temperature Results

		Original Length (L=15.85m)	**Original Length (L=15.85m)**	**Shortened Length (L=13.36m)**
	Mass Flow Rate $\dot{m}_r$ (kg/s)	0.000542	0.000536	0.000542
Temperature (°C)	Ambient T_{amb}	25.0	25.2	25.1
	Air Right Side $T_{a,right}$	25.7	26.1	25.9
	Condenser Inlet T_{in}	63.5	63.2	62.2
	Two Phase Region Inlet T_{satin}	42.5	45.0	41.5
	Two Phase Region Outlet T_{satout}	41.5	43.0	40.5
	Condenser Outlet T_{out}	40.0	36.1	40.0

5.1.2.1 Heat Transfer Rate Calculations

Heat transfer rates have been calculated with the help isobutane property tables and *P-h* diagram. An example *P-h* diagram can be found in Appendix C. Heat transfer rate results are shown in Table 5.3. It was observed that all of the condensers work with similar heat transfer rates. The major difference comes from the subcooled region heat transfer rates.

Table 5.3 Heat Transfer Rate Results

Heat Transfer Rate [W]		**Original Length (L=15.85m) 4.76 mm Outer Diameter**	**Original Length (L=15.85m) 4 mm Outer Diameter**	**Shortened Length (L=13.36m) 4.76 mm Outer Diameter**
$\dot{Q}_{desup}$	Desuperheating Region	23.83	22.68	23.29
$\dot{Q}_{two}$	Two Phase Region	171.17	166.62	171.44
$\dot{Q}_{sub}$	Subcooled Region	4.33	11.10	2.17
$\dot{Q}_{tot}$	Total	199.33	200.40	196.90

5.1.2.2 Inside Convective Heat Transfer Coefficient Calculations

The desuperheating region calculations have been performed using two different correlations, and similar results have been obtained. The two phase region heat transfer coefficient has been calculated using the correlation suggested by Cavallini-Zecchin. For the condensers of 4.76 mm tube outer diameters, the inside convective heat transfer coefficient values were lower compared to those for 4 mm outer diameter condensers. For the subcooled region, laminar flow assumption has been made. Fully developed conditions have been checked. Table 5.4 summarizes the inside convective heat transfer coefficient results.

Table 5.4 Inside Convective Heat Transfer Coefficient Results

Inside Convective Heat Transfer Coefficient [W/m^{2}K]		**Original Length (L=15.85m) 4.76 mm Outer Diameter**	**Original Length (L=15.85m) 4 mm Outer Diameter**	**Shortened Length (L=13.36m) 4.76 mm Outer Diameter**
h_{iDb} : Dittus Boelter Correlation	Desuperheating Region	416.86	510.85	416.12
h_{iG} : Gnielinski Correlation	Desuperheating Region	398.43	487.93	397.38
h_{iCZ} : Cavallini-Zecchin Correlation	Two Phase Region	2022.27	2428.07	2034.11
h_{iL}: Laminar Flow	Subcooled Region	102.53	106.87	167.98

5.1.2.3 Outside Convective Heat Transfer Coefficient Calculations

The air side convective heat transfer coefficient has been calculated with two different equations. Experimental data indicated that desuperheating takes place in the vertical part of the condenser tubes. In this region, the heat transfer coefficient has been calculated by dividing the corresponding heat transfer rates by the temperature difference. The saturation temperature for the 4 mm outer diameter

condenser was 2-3°C higher than that for 4.76 mm condensers. Hence, the outside convective heat transfer coefficient for the desuperheating region was smaller for condensers of 4 mm outer diameter tubes. For the two phase and subcooled regions, correlations from the literature have been used. Table 5.5 gives the results for the outside convective heat transfer coefficients.

Table 5.5 Outside Convective Heat Transfer Coefficient Results

Outside Convective Heat Transfer Coefficient [W/m^{2}K]		**Original Length (L=15.85m) 4.76 mm Outer Diameter**	**Original Length (L=15.85m) 4 mm Outer Diameter**	**Shortened Length (L=13.36m) 4.76 mm Outer Diameter**
h_{odesup}	Desuperheating Region	47.96	30.49	51.16
$h_{otwo\ and\ sub}$	Two Phase Region	16.09	17.22	16.81

5.1.2.4 *UA* and Overall Heat transfer Coefficient Results

The *UA* values and the overall heat transfer coefficient values have been calculated for each different region. In the desuperheating region, the *UA* value for 4 mm tubes was smaller than that for 4.76 mm tubes. For the two phase region, shortened length version tubes had greater *UA* values compared to the others. For the same thermal performance, it is possible to use condensers of 4 mm tube outer diameters, and those of 4.76 mm tube outer diameter with shortened tubes instead of wider and/or longer tubes. This is a desirable result requiring less material and yielding reduced cost. Table 5.6 lists the *UA* values for the investigated condensers.

Table 5.6 *UA* Results

***UA* [W/K]**		**Original Length (L=15.85m) 4.76 mm Outer Diameter**	**Original Length (L=15.85m) 4 mm Outer Diameter**	**Shortened Length (L=13.36m) 4.76 mm Outer Diameter**
UA_{desup}	Desuperheating Region	0.86	0.49	0.84
UA_{two}	Two Phase Region	9.13	8.86	10.18
UA_{sub}	Subcooled Region	0.92	1.21	0.28

In the desuperheating region, similar to *UA* values the overall heat transfer coefficient for 4 mm tubes was smaller than that for 4.76 mm tubes. For the two phase region, 4.76 mm tubes of the original length had a lower overall heat transfer coefficient compared to the others. Table 5.7 shows the overall heat transfer coefficient values of each region for the investigated condensers.

Table 5.7 Overall Heat Transfer Coefficient Results

Overall Heat Transfer Coefficient [W/m^{2}K]		**Original Length (*L*=15.85m) 4.76 mm Outer Diameter**	**Original Length (*L*=15.85m) 4 mm Outer Diameter**	**Shortened Length (*L*=13.36m) 4.76 mm Outer Diameter**
U_{desup}	Desuperheating Region	41.08	27.85	43.21
U_{two}	Two Phase Region	14.47	15.50	14.96
U_{sub}	Subcooled Region	8.89	9.06	10.39

5.1.3 Second Stage Refrigerator Test Results

After performing the solo condenser tests and observing almost the same overall heat transfer coefficient and *UA* results for original length 4 mm and shortened length 4.76 mm outer diameter tubes, in the last part of the study additional refrigerator energy consumption tests have been completed as final control experiments. Table 5.8 lists the results of the final control experiments (shaded green) as well as the previous results.

Table 5.8 Final Control Experiment Results

Experiment No	**Condenser Length**	**Condenser Outer Diameter (mm)**	**Condenser Inclination**	**Tube Orientation**	**Amount of Refrigerant (gr)**	**Daily Energy Measurement Results (kWh)**	**EEI Index Results**
1	Original	4	Yes	Horizontal	56	0.758	33.23
3	Original	4	No	Horizontal	56	0.788	34.55
6	Original	4.76	Yes	Horizontal	57	0.750	32.88
7	Original	4.76	No	Horizontal	57	0.776	34.02
17	Original	4	Yes	Horizontal	56	0.761	33.36
18	Original	4	No	Horizontal	56	0.788	34.55
19	Shortened	4.76	Yes	Horizontal	56	0.760	33.32
20	Shortened	4.76	No	Horizontal	56	0.776	34.02

After the completion of the second stage refrigerator experiments the following may be stated:

- Results for 4 mm tube outer diameter were almost the same as those in the first part of the experimental results,
- Condensers with 4.76 mm shortened tubes performed almost the same way as those with original tube length.
- 4.76 mm shortened tubes performed the same way as 4mm ones.
- It is possible to save material and reduce the production cost by using shorter tubes of 4.76 mm or tubes of 4 mm diameter without any loss in the thermal performance or increase in the energy consumption.

5.2 Discussion

For the calculation of the total overall heat transfer coefficient, two different approaches could be used. The first approach is adding all of the calculated *UA* results of each region and dividing it by the total outer surface area of the condenser.

$$U_{tot} = \frac{\sum UA_{o,sect}}{A_{o,tot}} \tag{5.2}$$

In the second approach, the measured $\dot{Q}_{tot}$ results are used. For the logarithmic mean temperature difference calculation, Equation 5.3 is used. In Figure 5.12, below the heat transfer model is given. $T_{a,in}$ and $T_{a,out}$ are the averages of each six thermocouple measurements. Since the two phase region dominates other regions, T_{sat} was chosen as the condenser temperature.

$$\Delta T_{\text{lm}} = \frac{T_{a,in} - T_{a,out}}{\ln\left(\frac{T_{sat} - T_{a,in}}{T_{sat} - T_{a,out}}\right)} \tag{5.3}$$

$$U_{tot} = \frac{\dot{Q}_{tot}}{A_{o,tot}\Delta T_{lm}} \tag{5.4}$$

The results of the two different approaches are given in Table 5.9. The results showed that the condensers of 4.76 mm outer diameter of shortened length yielded greater total overall heat transfer coefficients compared to other investigated condensers.

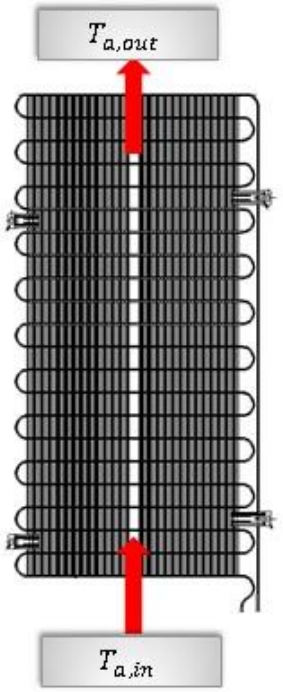

Figure 5.12 Heat transfer model for the total overall heat transfer coefficient.

Table 5.9 Total Overall Heat Transfer Coefficient Calculation Results

Total Overall Heat Transfer Coefficient [W/m^{2}K]	**Original Length (*L*=15.85m)**	**Original Length (*L*=15.85m)**	**Shortened Length (*L*=13.36m)**
	4.76 mm Outer Diameter	**4 mm Outer Diameter**	**4.76 mm Outer Diameter**
First Approach U_{tot}	14.52	14.67	15.63
Second Approach U_{tot}	15.32	14.47	16.77

CHAPTER 6

CONCLUSION

6.1 Conclusions

In the scope of this thesis, three different sets of experiments have been conducted. In the first and the third sets, a test chamber has been used to investigate the effects of different condenser configurations on refrigerator energy consumption. The test chamber was able to be kept the room temperature, the humidity level, and the air circulation stable during the experiments. In the second part of the study an experimental setup was used to investigate the performance characteristics of a variety of wire-and tube type refrigerator condensers. The setup was able to circulate a determined amount of refrigerant through the test condensers.

In the first part of the study, the experiments have been performed on the refrigerator to investigate the effects of different condenser combinations on the energy consumption. A DOE analysis indicated that

- the condenser inclination is the most effective condenser parameter for reducing the energy consumption;
- the condenser diameter and the refrigerant gas charge also have important effect for reducing the energy consumption;
- the condenser directional change affects the performance of condensers with 4mm tube diameter, but do not affect that for 4.76 mm diameter tubes;
- the change in condenser diameter have slight effect on the refrigerator energy consumption, however, it is important for the cost improvement.

In the second part of the study, the performance measurements for different condensers have been completed. The results showed that condensers with the original tube length with 4.00 mm and 4.76 mm outer diameter tubes, and the one of shortened length of 4.76 mm tube diameter yielded almost the same performances. For condensers of 4 mm tube diameter, due to reduced diameter, the change in the saturation temperature was high. For this reason, the outside heat transfer coefficient was lower than that for 4.76 mm tubes.

After conducting solo condenser tests, and observing almost the same overall heat transfer coefficient and *UA* results for 4 mm original length tubes and 4.76 mm shortened length tubes, in the last part of the study, additional refrigerator energy consumption tests have been completed. These results indicated that

- 4.76 mm outer diameter shortened length tubes yielded almost the same energy consumption and thermal performance with those of original length. However, considerable reduction in material (≈ 2.5 m less tube usage), hence, in weight (≈ 0.17 kg) and cost (≈ 0.4 Euro) may be accomplished with the use of shorter tubes.
- 4.76 mm diameter shortened length tubes yielded similar energy consumption results to those with 4 mm diameter tubes of the original length.

6.2 Recommendations for Future Work

As a continuation of this study, condensers with shortened tubes of 4.76 mm and 4 mm outer diameters may be tested on different types of refrigerators, such as on table top, no-frost, semi no-frost models.

In the present study, the angle of inclination was taken as 1.5°. Further analysis can be performed to investigate the effects of the inclination angle.

Forced cooled and mini channel type condensers are widely used in household appliances; further experiments may be expanded using such condensers.

According to the previous studies, [6, 7, 9] radiation has twenty to thirty percent contribution to the total heat transfer rate. In the present study radiative effects on condenser was not studied. For the further studies this effect may be investigated.

REFERENCES

[1]ENVER Enerji Verimliliği Derneği, Türkiye Enerji ve Enerji Verimliliği Çalışmaları Raporu, Temmuz 2010

[2] Bertoldi, P. ve Atanasiu, B. (2006). Electricity Consumption & Efficiency Trends in the enlarged European Union - Status Report 2006. European Commission Joint Research Centre. Ispra, Italia.

[3] Witzell, O.W. and Fontaine, W.E., "What are the Heat Transfer Characteristics of Wire and Tube Condensers?" Refrigerating Engineering, Vol. 65, pp. 33-37, 127, 1957.

[4] Witzell, O.W., Fontaine, W.E. and Papanek, W.J., "Convective Films Evaluated for Wire and Tube Heat Exchangers." ASHRAE Journal, Vol. 1, pp. 35-37, 127, 1959.

[5] Hoke, J.L., Clausing, A.M., Swofford, T.D., "An Experimental Investigation of Convective Heat Transfer Coefficient on Wire and Tube Refrigerator Condenser Coils.", ACRC TR-86, University of Illinois at Urbana-Campaign, IL., 1995.

[6] Tagliafico L. Tanda G.,"Radiation and Natural Convection Heat Transfer from Wire-and Tube Heat Exchangers in Refrigeration Appliances.", Int. J. Refrigeration, Vol.20, pp. 461-469, 1997.

[7] Okutucu, T., "Construction of a Test Setup for Experimental Evaluation of Refrigerator Condensers." M.S., Department of Mechanical Engineering, METU, 1999

[8] Bansal P.K., Chin T.C., "Modeling and Optimization of Wire-and-Tube Condenser.", Int. J. Refrigeration, Vol. 26, pp. 601-603, 2002.

[9] Dirgin, E., "Experimental Evaluation of Air-cooled Condensers for Household Refrigerators." M.S., Department of Mechanical Engineering, METU, 2002.

[10] Melo, C., Hermes, C.L., "A Heat Transfer Correlation for Natural Draft Wire-and-Tube Condensers." Int. J. Refrigeration, Vol. 32, pp. 546 –555, 2008.

[11] Hofmanas, I., Paukstaitis, L., "Numerical Heat Transfer Investigation of Wire-and-Tube Condenser." Mechanika, Vol. 18, pp. 82-87, 2012

[12] EU 1060/ 2010. "European Parliament and of the Council with regard to Energy Labelling of Household Refrigerating Appliances." Official Journal of the European Union, Brussels, 2010.

[13] ISO 15502. "Household Refrigerating Appliances, Characteristics and Test Methods." International Organization for Standardization, Cenevre, 2005.

[14] TS EN ISO 15502. "Evlerde Kullanılan Soğutma Cihazları - Karakteristikler ve Deney Metotları.", Türk Standartları Enstitüsü, Ankara, 2007.

[15] Incropera, F.P., et al. Fundamentals of Heat and Mass Transfer, Wiley, 6th Edition, USA. 2007.

[16] Sieder, E. N., Tate, G. E., Ind. Eng. Chem., 28, 1429, 1936.

APPENDIX A

CLIMATIC TEST CHAMBER and POWER ANALYZER CALIBRATION REPORTS

Table A.1 Sample Climatic Chamber Calibration Report

arçelik

ARCELİK A.Ş.
Buzdolabı İşletmesi

:50/50
07.05.2014

KALİBRASYON SERTİFİKASI
Calibration Certificate

Sayfa No :1/50
Page Number

Cihazın Sahibi ve Adresi *Customer*	:	ARÇELİK A.Ş
İstek Numarası *Order No.*	:	
Makine/Cihaz *Instrument/Device*	:	VERİ TOPLAMA İSTASYONLARI Oda 8 *Data acquisition systems Chamber 8*
İmalatçı *Manufacturer*	:	-
Tip *Type*	:	-
Seri Numarası *Serial Number*	:	285-9023-0011
Kalibrasyon Tarihi *Date of Calibration*	:	11.12.2013
Sertifikanın Sayfa Sayısı *Number of pages of the Certificate*	:	50

Bu kalibrasyon sertifikası, Uluslararası Birimler Sisteminde (SI) tanımlanmış birimleri realize eden ulusal ölçüm standartlarına izlenebilirliği belgeler.

This calibration certificate documents the traceabilty to national standarts, which realize the unit of measurement according to the International System of Units (SI).

Ölçüm sonuçları, genişletilmiş ölçüm belirsizlikleri ve kalibrasyon metodları bu sertifikanın tamamlayıcı kısmı olan takib eden sayfalarda verilmiştir.
The measurements, the uncertainties with confidence probability and calibration metods are given on the following pages which are part of this certificate.

Mühür *Seal*	**Tarih** *Date*	**Kalibrasyonu Yapan** *Calibrated by*	**Laboratuvar Müdürü** *Head of Calibration Laboratory*

Table A.1 Continues

Kalibrasyonda Kullanılan Referanslar *Refrences Used In Calibration*	:	**ÖLÇÜM CİHAZI**	**LABORATUVAR ENVANTER NO**	**İZLENEBİLİRLİK**
		FLUKE 5500 A MULTIFUNCTION CALIBRATOR	285-1382-001	NETES E12072947 07/12
Kalibrasyonu Yapılan Makina/Cihaz: *Deviced To Be Calibrated*		VERI TOPLAMA ISTASYONLARI Oda 8 *Data acquisition systems Chamber 8*		
Bulunduğu Yer *Place*	:			
Cihazın Laboratuvara Kabul Tarihi *Date of Receipt of Divece*	:	10.12.2012		
Kalibrasyon Talimatı *Calibration Direction*	:	GKA -19 _MKL VTS Kalibrasyon Talimatı		
Kalibrasyon Prosedürü *Calibration Procedur*	:	Kalıbrasyonu yapılmış kalıbratörden elde edılen değerler, gırış terminallerinden uygulanarak kalibratör değeri ile cihazın cihazın gösterge değerleri karşılaştırılmıştır.		
Olçüm Şartları *Measurements Conditions*	:	21,5 °C 46,4 % RH		
Çevre Şartları *Environmental Conditions*	:	21±2 °C 45 ±15 % RH		
Ölçüm Belirsizliği *Measurements Uncertainty*	:	Beyan edilen genişletilmiş ölçüm belirsizliği K=2 olarak alınan genişletme katsayısı ile çarpımı sonucunda bulunan değerdir. %95 oranında güvenirlik sağlamaktadır.		
Uygunluk Beyanı *Statement of Compliance*	:	Kalibrasyon sonrasında uygunluk kararı kullanıcının sorumluluğundadır.		
Açıklamalar *Remarks*	:	Kalibrasyon Sonucu sadece "Kalibrasyonu Yapılan Makina/Cihaz" bölümünde yer alan cihaza ait olup, kalibrasyon tarihinden itibaren ve sertifikada belirtilmiş olan şartlar altında geçerlidir. Bu sertifikada verilen sonuçlar, cihazın kalibrasyon tarihindeki durumuna ait olup, cihazın uzun dönem kararlılığı ile ilgili anlam taşımazlar.		
Kalibrasyon Etiketinin Yeri *Placement of the Calibration Label*	:	Cihazın üst yüzeyine yapıştırılmıştır.		

Table A.2 Sample Calibration Report of Temperature Measurement Results

Ölçüm Sonuçları:
Measurements Results

Sıcaklık Ölçümleri (°C) : İSTASYON 1
Temprature Measruments (°C) : STATION 1

1. Kanal *1.Chanel*

Uygulanan Değer *Applied Value*	**Okunan Değer** *Indicated Value*	**Alt Sınır** *Low Limit*	**Üst Sınır** *High Limit*	**Hata** *Error*	
-40 °C	-39,88 °C	-40,15 °C	-39,85 °C	0,12 °C	✓
-20 °C	-19,94 °C	-20,15 °C	-19,85 °C	0,06 °C	✓
0 °C	0,06 °C	-0,15 °C	0,15 °C	0,06 °C	✓
15 °C	15,03 °C	14,85 °C	15,15 °C	0,03 °C	✓
50 °C	49,97 °C	49,85 °C	50,15 °C	-0,03 °C	✓
100 °C	99,90 °C	99,85 °C	100,15 °C	-0,10 °C	✓
150 °C	149,94 °C	149,85 °C	150,15 °C	-0,06 °C	✓

Tablo A.3 Sample Calibration Report of Voltage and Current Measurement Results

Ölçüm Sonuçları:
Measurements Res

AC Gerilim (50Hz) İSTASYON 3
AC Voltage (50Hz) : STATION 3

Uygulanan Değer *Applied Value*	**Okunan Değer** *Indicated Value*	**Alt Sınır** *Low Limit*	**Üst Sınır** *High Limit*	**Hata** *Error*	**Ölçüm Belirsizliği** *Measurement Unc.*	
150 V	150,18 V	149,50 V	150,50 V	0,18 V	1,83E-02	✓
230 V	229,70 V	229,50 V	230,50 V	-0,30 V	2,70E-02	✓
300 V	299,80 V	299,50 V	300,50 V	-0,20 V	3,50E-02	✓

AC Akım (50 Hz) İSTASYON 3
AC Current (50Hz) : STATION 3

Uygulanan Değer *Applied Value*	**Okunan Değer** *Indicated Value*	**Alt Sınır** *Low Limit*	**Üst Sınır** *High Limit*	**Hata** *Error*	**Ölçüm Belirsizliği** *Measurement Unc.*	
0,10 A	0,10 A	0,09 A	0,11 A	0,00 A	1,28E-04	✓
0,30 A	0,30 A	0,29 A	0,31 A	0,00 A	2,06E-04	✓
0,50 A	0,50 A	0,49 A	0,51 A	0,00 A	2,70E-04	✓
0,75 A	0,75 A	0,74 A	0,76 A	0,00 A	3,51E-04	✓
1,50 A	1,50 A	1,49 A	1,51 A	0,00 A	6,95E-04	✓
2,00 A	2,00 A	1,99 A	2,01 A	0,00 A	2,89E-03	✓
2,50 A	2,50 A	2,49 A	2,51 A	0,00 A	7,73E-04	✓
3,00 A	3,00 A	2,99 A	3,01 A	0,00 A	1,81E-04	✓

Tablo A.4 Sample Calibration Report of Power and AC Power Consumption Results

Ölçüm Sonuçları:
Measurements Results

Güç (50-60) Hz İSTASYON 2
Power (50-60Hz) : STATION 2

Uygulanan Değer *Applied Value*	**Okunan Değer** *Indicated Value*	**Alt Sınır** *Low Limit*	**Üst Sınır** *High Limit*	**Hata** *Error*	
1 W 230V 50 Hz	1,00 W	0,99 W	1,01 W	0,00 W	✓
5 W 230V 50 Hz	5,01 W	4,95 W	5,05 W	0,01 W	✓
50 W 230V 50 Hz	50,05 W	49,50 W	50,05 W	0,05 W	✓
100 W 230V 50 Hz	100,08 W	99,00 W	101,00 W	0,08 W	✓
1 W 230V 60 Hz	1,01 W	0,99 W	1,01 W	0,01 W	✓
100 W 230V 60 Hz	100,10 W	99,00 W	101,00 W	0,10 W	✓
1 W 110V 60 Hz	0,99 W	0,99 W	1,01 W	-0,01 W	✓
100 W 110V 60 Hz	100,01 W	99,00 W	101,00 W	0,01 W	✓
900 W 110V 60 Hz	899,9 W	891,00 W	909,00 W	-0,10 W	✓

AC Güç Tüketimi İSTASYON 2
AC Power Consumption Station 2

Uygulanan Değer *Applied Value*	**Okunan Değer** *Indicated Value*	**Alt Sınır** *Low Limit*	**Üst Sınır** *High Limit*	**Hata** *Error*	
1 Wh 230V 50 Hz	1,00 Wh	0,99 Wh	1,01 Wh	0,00	✓
5 Wh 230V 50 Hz	5,02 Wh	4,95 Wh	5,05 Wh	0,02	✓
50 Wh 230V 50 Hz	50,03 Wh	49,50 Wh	50,05 Wh	0,03	✓
100 Wh 230V 50 Hz	100,08 Wh	99,00 Wh	101,00 Wh	0,08	✓
1 Wh 230V 60 Hz	1,01 Wh	0,99 Wh	1,01 Wh	0,01	✓
100 Wh 230V 60 Hz	100,10 Wh	99,00 Wh	101,00 Wh	0,10	✓
1 Wh 110V 60 Hz	1,00 Wh	0,99 Wh	1,01 Wh	0,00	✓
100 Wh 110V 60 Hz	100,05 Wh	99,00 Wh	101,00 Wh	0,05	✓
900 Wh 110V 60 Hz	900,15 Wh	891,00 Wh	909,00 Wh	0,15	✓

APPENDIX B

SAMPLE SOLO CONDENSER PERFORMANCE CALCULATIONS

Table B.1 Condenser Geometric Properties

	Condenser Geometric Properties
Tube Outer Diameter $D_{t,out}$ (mm)	**4.76**
Tube Inner Diameter $D_{t,in}$ (mm)	3.36
Tube Spacing S_t (mm)	60
Number of Passes, n_t	22
Total Tube Length L_t (mm)	15850
Wire Diameter D_w (mm)	1.3
Wire Length L_w (mm)	1260
Number of Wires n_w	108
Wire Spacing S_w (mm)	10
Wire Perimeter P_w (mm)	4.084
Width of Condenser W (mm)	630
Height of Condenser H (mm)	1260

$$A_{t,out} = \pi D_{t,out}(L_t - n_t n_w D_w) = 0.191 \text{ m}^2$$

$$A_w = \pi n_w D_w L_w = 0.554 \text{ m}^2$$

$$A_{o,tot} = A_{t,out} + A_w = 0.747 \text{ m}^2$$

Table B.2 Length of Different Regions

Desuperheating Region Length $L_{t,desup}$ (m)	1.40
Two Phase Region Length $L_{t,two}$ (m)	12.40
Subcooled Region Length $L_{t,sub}$ (m)	2.05

$$A_{t,insup} = \pi D_{t,in} L_{t,sup} = 0.015 \text{ m}^2$$

$A_{t,intwo} = \pi D_{t,in} L_{t,two}$= 0.131 m^2

$A_{t,insub} = \pi D_{t,in} L_{t,sub}$= 0.022 m^2

$A_{t,outsup} = \pi D_{t,out} L_{t,sup}$= 0.021 m^2

$A_{t,outtwo} = \pi D_{t,out} L_{t,two}$= 0.149 m^2

$A_{t,outsub} = A_{t,out} - \left(A_{t,outsup} + A_{t,outtwo}\right)$= 0.021 m^2

$A_{w,two} = A_w L_{t,two} / L_t$= 0.477 m^2

$A_{w,sub} = A_w - A_{w,two}$= 0.079 m^2

Table B.3 Condenser and Climatic Chamber Temperature Details

T_{amb} (°C)	25
$T_{a,right}$ (°C) Condenser Right Side	25.7
T_{in} (°C)	63.5
T_{satin} (°C)	42.5
T_{satout} (°C)	41.5
T_{out} (°C)	40
m_r : Mass Flow Rate (kg/s)	0.000542

For the desuperheating region, properties were calculated at mean temperature ((T_{in}+T_{satin})/2) Detailed isobutane refrigerant psychical properties can be found in Appendix D.

Table B.4. Desuperheating Region Refrigerant Properties

μ_v: Dynamic Viscosity of Vapor Phase Refrigerant (Pa.s)	0.00000874
k_v : Thermal Conductivity of Refrigerant in Vapor Phase (W/mK)	0.02
C_{pv} :Specific Heat of the Refrigerant (J/kgK)	2070

Calculation of Heat Transfer Rates:

$\dot{Q}_{sup} = \dot{m}_r\left(h_{in} - h_g\right) = 23.83\ W$

$\dot{Q}_{two} = \dot{m}_r h_{fg} = 171.17\ W$

$$\dot{Q}_{sub} = \dot{m}_r\left(h_f - h_{out}\right) = 4.33\ W$$

$$\dot{Q} = \dot{Q}_{sup} + \dot{Q}_{two} + \dot{Q}_{sub} = 199.33\ W$$

Calculation of Inside Convective Heat Transfer Coefficients:

$$Re_D = \frac{4\dot{m}_r}{\pi D_{t,in}\mu} = 23485$$

For Desuperheating Region (Turbulance Flow Re>2300) from Dittus-Boelter Equation

$$h_{i,\,Db} = \frac{k_v}{d_{t,in}} 0.023 \left(\frac{4\dot{m}_r}{\pi d_{t,in}\mu_v}\right)^{0.8} \left(\frac{\mu_v c_{pv}}{k_v}\right)^{0.3} = 416.86\ \mathrm{W/m^2K}$$

Also Gnielinski Correlation

$$f = (0.79 \ln Re - 1.64)^{-2} = 0.0251$$

$$h_{i,G} = \frac{k}{d_{t,in}} \frac{\frac{f}{8}(Re-1000)Pr}{1+12.7\left(\frac{f}{8}\right)^{0.5}\left(Pr^{2}/_{3}-1\right)} = 398.43\ \mathrm{W/m^2K}$$

For the two phase region, properties were calculated at the saturation temperature (T_{sat}) as

Table B.5 Two Phase Region Refrigerant Properties

μ_l: Dynamic Viscosity of Liquid Phase Refrigerant (Pa.s)	0.0001259
k_l : Thermal Conductivity of Refrigerant in Liquid Phase (W/mK)	0.0884
Cp_l :Specific Heat of the Refrigerant (kJ/kgK)	2576
μv: Dynamic Viscosity of Vapor Phase Refrigerant (Pa.s)	0.00000833
kv : Thermal Conductivity of Refrigerant in Vapor Phase (W/mK)	0.0186
Cpv :Specific Heat of the Refrigerant (kJ/kgK)	1964

For the two phase from the correlation suggested by Cavallini and Zecchin,

$$Re_l = \frac{4\dot{m}(1-x)}{\pi d_{t,in}\mu_l} \qquad Re_v = \frac{4\dot{m}x}{\pi d_{t,in}\mu_v}$$

$$Re_{eq} = Re_l + Re_v \frac{\mu_v}{\mu_l}\left(\frac{\rho_l}{\rho_v}\right)^{0.5}$$

$$h_{i,Cz} = \frac{k_l}{d_{t,in}} 0.05 Re_{eq}^{0.8} \left(\frac{\mu_l c_{pl}}{k_l}\right)^{0.33}$$

For every x values with 0.1 increments below table was generated

Table B.6 Cavallini and Zecchin Correlation, Equivalent Reynolds Number Calculations

For 4,76mm Pipe @42°C Saturation				
x	Re_l: Reynolds Number	Re_v: Reynolds Number	Re_{eq}: Reynolds Number	h_{iCZ} (W/m^2K)
0	1630.34	0	1630.34	750.23
0.1	1467.30	2464.1	2456.52	1041.43
0.2	1304.27	4928.19	3282.70	1313.28
0.3	1141.24	7392.29	4108.88	1571.64
0.4	978.2	9856.39	4935.06	1819.73
0.5	815.17	12320.49	5761.25	2059.62
0.6	652.13	14784.58	6587.43	2292.70
0.7	489.1	17248.68	7413.61	2519.98
0.8	326.06	19712.78	8239.8	2742.25
0.9	163.03	22176.88	9065.98	2960.09
1	0	24640.98	9892.16	3174
			h_{icz} Average	2022.27

For the subcooled region laminar flow assumption was made. Fully developed condition was checked. For the subcooled region, properties were calculated at mean temperature ((T_{satout}+T_{out})/2)

Table B.7 Subcooled Region Refrigerant Properties

μ_s: Dynamic Viscosity of Refrigerant (Pa.s)	0.0001511
μ_l: Dynamic Viscosity of Liquid Phase Refrigerant (Pa.s)	0.0001272
k_l : Thermal Conductivity of Refrigerant in Liquid Phase (W/mK)	0.089
Cp_l :Specific Heat of the Refrigerant (kJ/kgK)	2568

Equation (4.14) suggested by Sieder and Tate [16] is valid for $0.60 \leq Pr \leq 5$ and $0.0044 \leq (\mu/\mu_s) \leq 9.75$. If $\overline{Nu_D}$ falls below 3.66, it is reasonable to use $\overline{Nu_D} = 3.66$, since the fully developed conditions are valid.

$$Pr = {C_p\mu}/{k} = 3.67$$

$$Re_D = \frac{4\dot{m}_r}{\pi D_{t,in}\mu} = 1614.67$$

$$\overline{Nu_D} = \frac{h_{i,Lam}d_{t,in}}{k_l} = 1.86\left(\frac{Re_D Pr}{L/d_{t,in}}\right)^{1/3}\left(\frac{\mu}{\mu_s}\right)^{0.14} = 3.871$$

$$h_{i,L} = \frac{k_l}{d_{t,in}}3.871 = 102.53\ \mathrm{W/m^2K}$$

Calculation of Outside Convective Heat Transfer Coefficients:

Table B.8 Air Physical Properties

k_{air}: Thermal conductivity of air at T_{amb}(W/mK)	0.026
ρ_{air}: Density of air at T_{amb} (kg/m^3)	1.171
μ_{air}: Dynamic viscosity of air at T_{amb}(Pa.s)	0.0000183

$$h_o = \frac{\frac{\dot{Q}_{sup}}{T_{in}-T_{sat}}}{A_t\ln\left({T_{in}-T_\infty}/{T_{sat}-T_\infty}\right)} = 47.96\ \mathrm{W/m^2K}$$

$$T_{amb} = \frac{T_{a,down} + T_{a,up} + T_{a,left} + T_{a,right}}{4} = 25°C$$

$$\beta = \frac{1}{\left(\frac{(T_{satin} + T_{amb})}{2} + 273.15\right)} = 0.003$$

$$D_c = \frac{\frac{S_w}{S_t} d_0^2 + d_w^2}{\frac{S_w}{S_t} d_0 + d_w} = 2.611 \text{ mm}$$

$$Gr = \frac{{d_c}^3 \rho_a^2 g \beta (T_{satin} - T_{amb})}{\mu_a^2} = 247.15$$

$$Nu = 0.4724 Gr^{0.2215} = 1.601$$

$$h_o = \frac{Nuk_a}{D_c} = 16.09 \text{ W/m}^2\text{K}$$

Calculation of Overall Heat Transfer Coefficients:

Table B.9 Tube and Wire Thermal Conductivities

k_t: Tube thermal conductivity (W/mK)	45
k_w: Wire thermal conductivity (W/mK)	45

$$U_{sup} = \frac{\dot{Q}_{sup}}{A_{t,outsup} \Delta T_{lm,amb}}$$

$$\frac{1}{UA_{sup}} = \frac{1}{h_{isup} A_{\text{t,indesup}}} + \frac{\ln(D_{\text{t,out}}/D_{\text{t,in}})}{2\pi k_t L_t} + \frac{1}{h_{o,sup} \text{A}_{\text{t,outdesup}}}$$

$$UA_{sup} = 0.86 \text{ W/K}$$

The fin efficiency can be obtained using

$$\eta_f = \frac{\tanh\left(mS_t/2\right)}{m\frac{S_t}{2}} = 0.92$$

$$U_{two} = \frac{\dot{Q}_{\text{two}}}{A_{\text{t,outtwo}}\Delta T_{lm,amb}}$$

$$\frac{1}{UA_{two}} = \frac{1}{h_{itwo}A_{\text{t,intwo}}} + \frac{\ln(D_{\text{t,out}}/D_{\text{t,in}})}{2\pi k_t L_t} + \frac{1}{h_o(A_{\text{t,outtwo}}+\eta_f A_{\text{wtwo}})}$$

$$UA_{two} = 9.13 \text{ W/K}$$

$$U_{sub} = \frac{\dot{Q}_{sub}}{A_{\text{t,outsub}}\Delta T_{lm,amb}}$$

$$\frac{1}{UA_{sub}} = \frac{1}{h_{isub}A_{t,\text{insub}}} + \frac{\ln(D_{\text{t,out}}/D_{\text{t,in}})}{2\pi k_t L_t} + \frac{1}{h_o(A_{\text{t,outsub}} + \eta_f A_{wsub})}$$

$$UA_{\text{sub}} = 0.92 \text{ W/K}$$

Calculation of Total Overall Heat Transfer Coefficients:

For the calculation of total overall heat transfer coefficient two different approaches were used. The first approach is adding all of the calculated *UA* results of each region and dividing by total outer surface area of the condensers.

$$U_{tot} = \frac{\sum UA_{o,sect}}{A_{o,tot}} = 14.52 \text{ W/m}^2\text{K}$$

In the second approach calculated $\dot{Q}_{tot}$ results were used. For the log mean temperature difference below equation was used. $T_{a,in}$ and $T_{a,out}$ are the averages of each six thermocouple measurements. Since two phase region dominates other regions T_{sat} temperature was chosen as the condenser temperature.

Table B.10 Airside Average Temperature Measurements

Air Inlet Average Temperature $\boldsymbol{T_{a,in}}$(°C)	24.486
Air Outlet Average Temperature $\boldsymbol{T_{a,ut}}$(°C)	24.661

$$\Delta T_{\mathrm{lm}} = \frac{T_{a,in} - T_{a,out}}{\ln\left(\frac{T_{T,sat} - T_{a,in}}{T_{T,sat} - T_{a,out}}\right)} = 17.43 \text{ K}$$

$$U_{tot} = \frac{\dot{Q}_{tot}}{A_{o,tot}\Delta T_{lm}} = 15.32 \text{ W/m}^2\text{K}$$

APPENDIX C

SAMPLE CONDENSATION LINE DRAWING ON *P-h* diagram

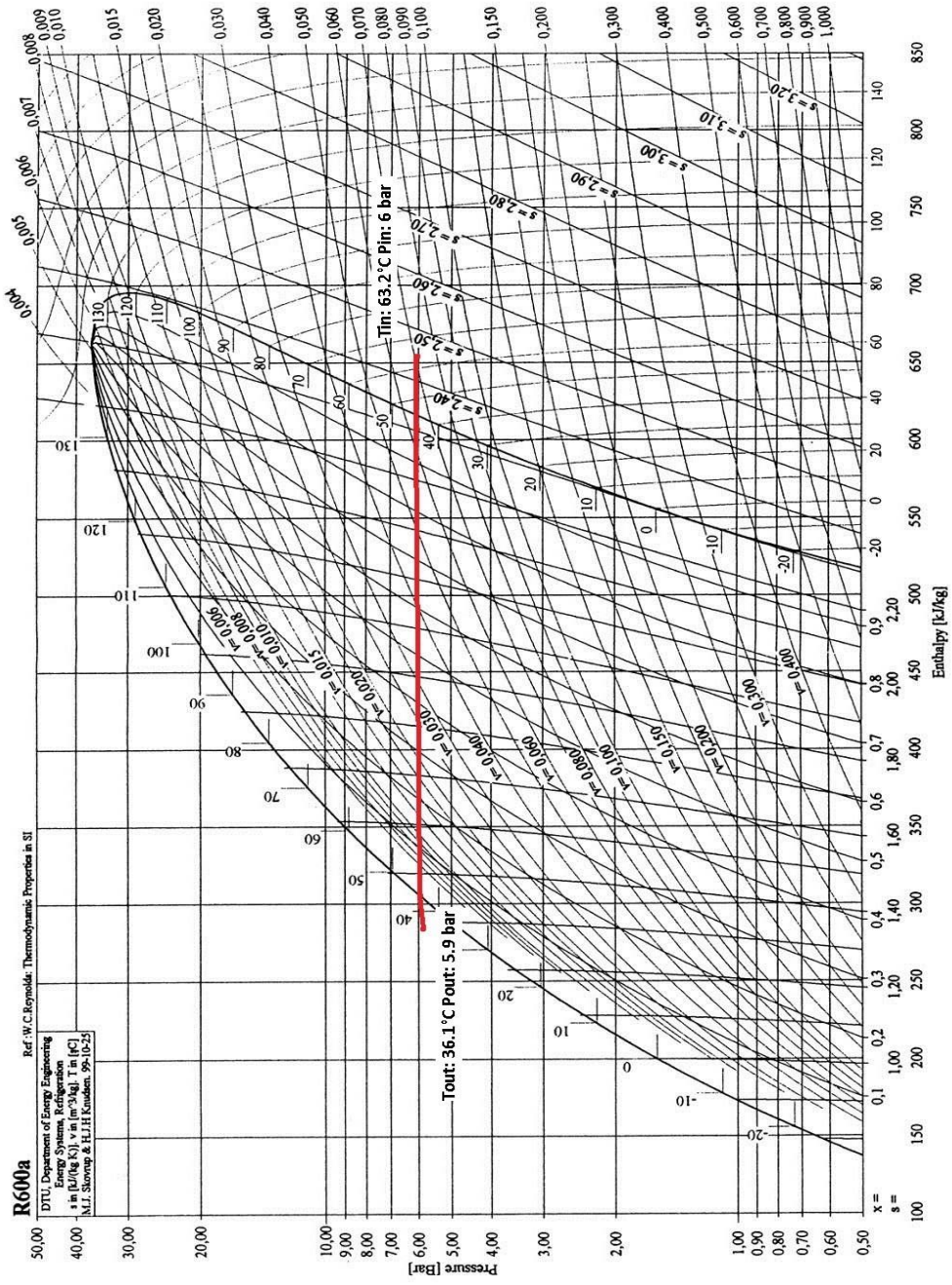

Figure C.1 Sample condensation line drawing on isobutane *P-h* diagram

APPENDIX D

ISOBUTANE (R600a) PHYSICAL PROPERTIES

Table D.1 Isobutane Physical Properties

	Temperature (°C)	Pressure (atm)	Liquid Density (kg/m³)	Vapor Density (kg/m³)	Liquid Enthalpy (kJ/kg)	Vapor Enthalpy (kJ/kg)	Liquid Entropy (kJ/kg-K)	Vapor Entropy (kJ/kg-K)	Liquid Cp (kJ/kg-K)	Vapor Cp (kJ/kg-K)	Liquid Therm. Cond. (mW/m-K)	Vapor Therm. Cond. (mW/m-K)	Liquid Viscosity (µPe-s)	Vapor Viscosity (µPe-s)	Liquid Kin. Viscosity (cm²/s)	Vapor Kin. Viscosity (cm²/s)	Liquid Prandtl
1	-80,000	0,022408	664,46	0,082374	31,823	451,39	0,27587	2,4481	1,9441	1,2121	131,92	7,5028	619,23	4,9072	0,0093193	0,59572	9,1255
2	-75,000	0,032852	659,53	0,11782	41,587	457,40	0,32578	2,4242	1,9613	1,2330	129,83	7,8847	565,33	5,0331	0,0085716	0,42718	8,5400
3	-70,000	0,047129	654,58	0,16504	51,439	463,48	0,37487	2,4031	1,9789	1,2543	127,73	8,2724	518,15	5,1585	0,0079157	0,31256	8,0277
4	-65,000	0,066268	649,60	0,22678	61,380	469,63	0,42319	2,3845	1,9969	1,2761	125,61	8,6657	476,59	5,2832	0,0073366	0,23297	7,5766
5	-60,000	0,091472	644,58	0,30616	71,413	475,86	0,47080	2,3683	2,0153	1,2983	123,48	9,0647	439,76	5,4073	0,0068225	0,17662	7,1773
6	-55,000	0,12412	639,53	0,40667	81,540	482,14	0,51774	2,3541	2,0342	1,3211	121,35	9,4691	406,97	5,5308	0,0063635	0,13600	6,8220
7	-50,000	0,16577	634,44	0,53214	91,764	488,49	0,56405	2,3419	2,0536	1,3444	119,23	9,8790	377,61	5,6536	0,0059518	0,10624	6,5041
8	-45,000	0,21818	629,30	0,68678	102,09	494,89	0,60976	2,3315	2,0735	1,3683	117,10	10,294	351,21	5,7758	0,0055810	0,084100	6,2189
9	-40,000	0,28327	624,12	0,87513	112,51	501,35	0,65491	2,3227	2,0941	1,3929	114,99	10,715	327,39	5,8975	0,0052455	0,067390	5,9621
10	-35,000	0,36316	618,89	1,1021	123,04	507,85	0,69955	2,3154	2,1152	1,4183	112,88	11,141	305,80	6,0187	0,0049411	0,054612	5,7301
11	-30,000	0,46013	613,61	1,3729	133,68	514,40	0,74369	2,3095	2,1369	1,4443	110,79	11,573	286,17	6,1395	0,0046637	0,044719	5,5198
12	-25,000	0,57663	608,27	1,6931	144,43	520,99	0,78738	2,3048	2,1593	1,4712	108,71	12,011	268,27	6,2600	0,0044104	0,036973	5,3288
13	-20,000	0,71530	602,88	2,0687	155,30	527,61	0,83064	2,3013	2,1824	1,4989	106,65	12,454	251,90	6,3803	0,0041783	0,030842	5,1548
14	-15,000	0,87889	597,41	2,5060	166,29	534,26	0,87351	2,2989	2,2063	1,5275	104,61	12,904	236,88	6,5007	0,0039651	0,025940	4,9960
15	-10,000	1,0703	591,88	3,0117	177,40	540,93	0,91601	2,2975	2,2309	1,5570	102,59	13,361	223,07	6,6213	0,0037688	0,021985	4,8508
16	-5,0000	1,2926	586,27	3,5928	188,63	547,63	0,95816	2,2969	2,2564	1,5875	100,60	13,826	210,33	6,7424	0,0035876	0,018766	4,7177
17	0,00000	1,5490	580,58	4,2570	200,00	554,34	1,0000	2,2972	2,2827	1,6191	98,632	14,299	198,56	6,8642	0,0034201	0,016125	4,5955
18	5,0000	1,8428	574,80	5,0121	211,50	561,06	1,0415	2,2983	2,3100	1,6517	96,695	14,781	187,66	6,9870	0,0032649	0,013940	4,4831
19	10,000	2,1773	568,92	5,8670	223,15	567,78	1,0828	2,3000	2,3382	1,6856	94,788	15,273	177,54	7,1112	0,0031207	0,012121	4,3796
20	15,000	2,5561	562,95	6,8308	234,94	574,50	1,1239	2,3023	2,3676	1,7208	92,913	15,776	168,12	7,2372	0,0029865	0,010595	4,2842
21	20,000	2,9827	556,86	7,9134	246,88	581,21	1,1647	2,3051	2,3982	1,7573	91,071	16,292	159,34	7,3654	0,0028614	0,0093075	4,1959
22	25,000	3,4608	550,65	9,1258	258,98	587,90	1,2053	2,3085	2,4300	1,7955	89,262	16,823	151,13	7,4965	0,0027445	0,0082145	4,1142
23	30,000	3,9943	544,31	10,480	271,24	594,57	1,2458	2,3123	2,4633	1,8353	87,489	17,371	143,43	7,6308	0,0026351	0,0072815	4,0385
24	35,000	4,5869	537,83	11,988	283,67	601,21	1,2861	2,3165	2,4982	1,8771	85,752	17,937	136,20	7,7693	0,0025324	0,0064607	3,9680
25	40,000	5,2426	531,19	13,666	296,28	607,80	1,3263	2,3211	2,5349	1,9210	84,051	18,524	129,39	7,9125	0,0024359	0,0057899	3,9024
26	45,000	5,9654	524,37	15,529	309,07	614,34	1,3664	2,3259	2,5737	1,9675	82,387	19,136	122,96	8,0616	0,0023449	0,0051914	3,8412
27	50,000	6,7594	517,37	17,595	322,06	620,82	1,4064	2,3309	2,6148	2,0167	80,761	19,777	116,87	8,2176	0,0022589	0,0046703	3,7839